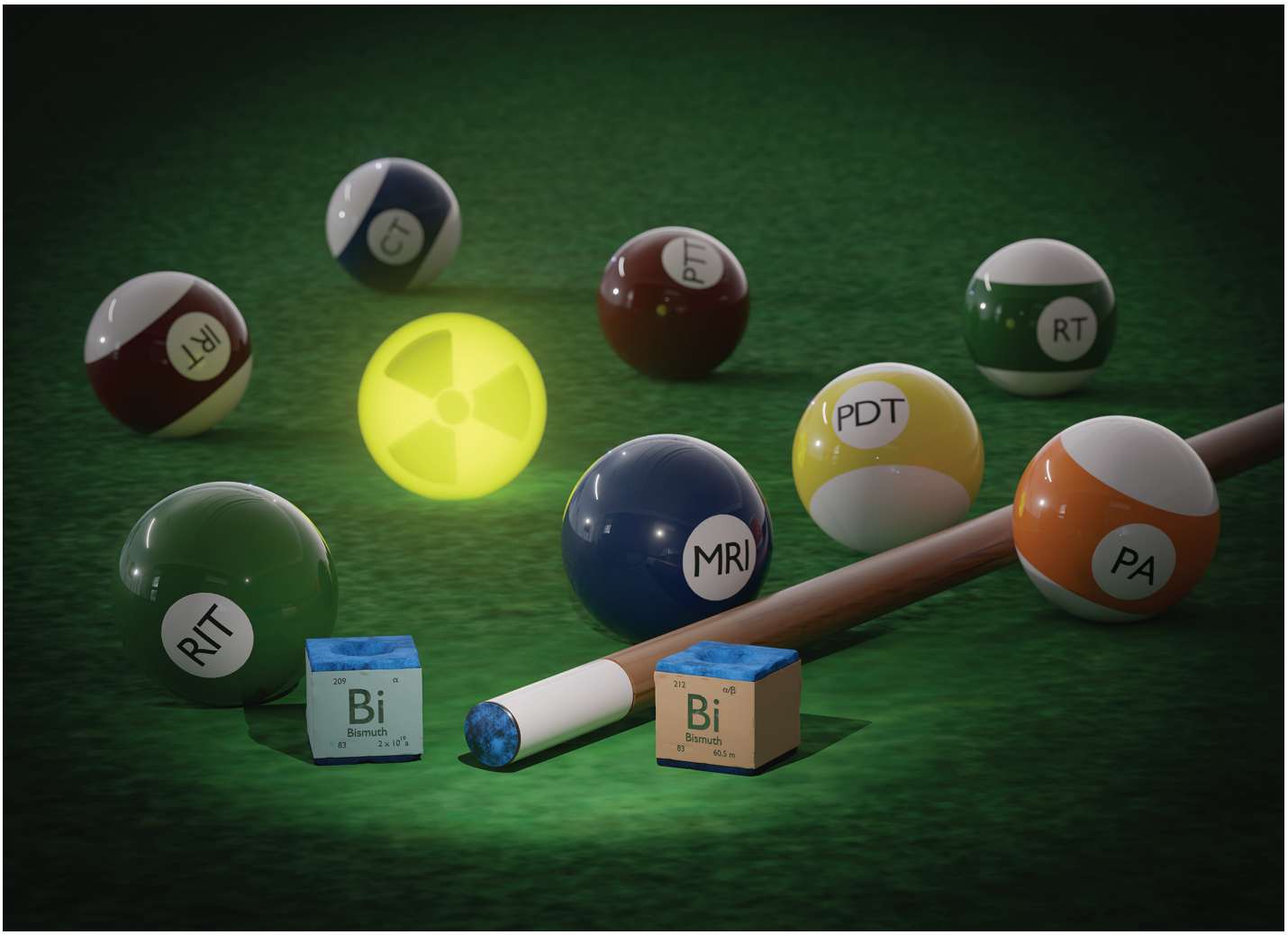

Showcasing research and a perspective view from Professor Philip Andrew's laboratory, School of Chemistry, Monash University, Melbourne, Australia and Professor Michael Bachmann's and Dr Holger Stephan's laboratories, Institute of Radiopharmaceutical Cancer Research, Helmholtz-Zentrum Dresden-Rossendorf, Dresden, Germany.

Targeted bismuth-based materials for cancer

This Perspective summarises recent developments in bismuth-based materials, with a focus on cancer imaging and treatment. These new materials open up great prospects for improved imaging based on X-ray computed tomography (CT), photoacoustic imaging (PA), infrared thermography (IRT) and magnetic resonance imaging (MRI), as well as for efficient treatment options, in particular through photothermal therapy (PTT), photodynamic therapy (PDT) and radiation therapy (RT). New strategies that combine immunotherapy (IT) and radionuclide therapy (RIT) represent a particularly promising strategy for the future.

The authors would like to express their sincere thanks to Dr. Bernd Schröder (HZDR) for creating the cover.

Image reproduced by permission of HZDR – Bernd Schröder from *Dalton Trans.*, 2025, **54**, 5614.

As featured in:

See Holger Stephan *et al.*, *Dalton Trans.*, 2025, **54**, 5614.

Dalton Transactions

ROYAL SOCIETY OF CHEMISTRY

PERSPECTIVE

View Article Online
View Journal | View Issue

Cite this: *Dalton Trans.*, 2025, **54**, 5614

Targeted bismuth-based materials for cancer

Amna Batool,[a,b] Ina Kopp,[b] Manja Kubeil,[b] Michael Bachmann,*[b] Philip C. Andrews *[a] and Holger Stephan *[b]

Received 21st January 2025,
Accepted 23rd February 2025

DOI: 10.1039/d5dt00163c

rsc.li/dalton

The use of bismuth and its compounds in biomedicine has developed rapidly in recent years. Due to their unique properties, there are great opportunities for the development of new non-invasive strategies for the early diagnosis and effective treatment of cancers. This perspective highlights key fabrication methods to generate well-defined and clinically relevant bismuth materials of varying characteristics. On the one hand, this opens up a wide range of possibilities for unimodal and multimodal imaging. On the other hand, effective treatment strategies, which are increasingly based on combinatorial therapies, are given a great deal of attention. One of the biggest challenges remains the selective tumour targeting, whether active or passive. Here we present an overview on new developments of bismuth based materials moving forward from a simple enrichment at the tumour site *via* uptake by the mononuclear phagocytic system (MPS) to a more active tumour specific targeting *via* covalent modification with tumour-seeking molecules based on either small or antibody-derived molecules.

1. Introduction

Bismuth and many of its compounds are of great interest for medical applications due to their low toxicity.[1] This behaviour is particularly influenced by the stabilising ligands, the dosage form and the administered concentration.[2] The solubility of most bismuth compounds is low even in the acidic environment of the stomach and thus an almost complete elimination *via* the gastrointestinal tract is considered a crucial factor for low toxicity *in vivo*.[3] This has driven forward, in particular, the development of antimicrobial and antiparasitic metallodrugs, such as bismuth subsalicylate, colloidal bismuth subcitrate or ranitidine bismuth citrate.[4–6] Interactions with iron-containing proteins such as transferrin and lactoferrin as well as with various enzymes such as ureases, hydrogenases and ATPase are discussed as the underlying mechanisms of the biological

[a]*School of Chemistry, Monash University, Clayton, Melbourne, VIC 3800, Australia. E-mail: phil.andrews@monash.edu*
[b]*Institute of Radiopharmaceutical Cancer Research, Helmholtz-Zentrum Dresden-Rossendorf, Bautzner Landstrasse 400, 01328 Dresden, Germany. E-mail: m.bachmann@hzdr.de, phil.andrews@monash.edu, h.stephan@hzdr.de*

Amna Batool

Amna Batool is a doctoral researcher at the School of Science, Monash University specialising in nanobiotechnology and cancer theranostics. Her work focuses on the development and application of functionalised nanomaterials for biomedical use. Through the MHELTHERA collaboration at HZDR (Germany), she has engineered nanoparticles to investigate their potential in tumour-targeted diagnostics and therapy. Passionate about bridging nanotechnology and immunotherapy, Amna's research seeks to advance novel nanotechnology-based strategies for clinically relevant cancer research.

Ina Kopp

Ina Kopp studied chemistry at the University of Paderborn, wrote her thesis at the University of Innsbruck in 2021and is now a doctoral researcher at the Institute of Radiopharmaceutical Cancer Research at Helmholtz-Zentrum Dresden-Rossendorf (HZDR). Her work focuses on the development of novel bispidine chelators for radiopharmaceutical applications and multimodal imaging. As part of the MHELTHERA project, she was working on the detection of activated platelets at the Alfred Hospital and Monash Biomedical Imaging (MBI) in Melbourne, Australia.

activity of bismuth compounds.[7] The specific interactions of bismuth compounds with biologically active molecules has also initiated studies of the anticancer activity of both small and nanoscale materials.[8–12] With regard to small bismuth-based compounds, complexes with halide, nitrate, carboxylate and dithiocarbamate ligands as well as various heterocyclic compounds dominate. The majority of the investigations are limited to *in vitro* studies on cell toxicity.[13–27] In contrast, *in vivo* studies in connection with bismuth complexes that show anticancer activity are only just beginning.[28,29]

This also applies to the structural elucidation of the bismuth complexes used in solution. For example, bismuth complexes with oxido ligands tend to form larger clusters, linking them to nanoscale bismuth-based systems, which are being actively investigated for cancer imaging and therapy.[2,30–34] These new materials reveal great prospects in terms of improved imaging based on X-ray computed tomography (CT),[35] photoacoustic imaging (PA),[36] and infrared thermography (IRT),[37,38] as well as efficient treatment options using in particular photothermal therapy (PTT),[36] photodynamic therapy (PDT)[39] and radiotherapy (RT).[40,41] With regard to the latter, *i.e.* the application of external ionising radiation, there are promising developments to improve the treatment effectiveness of tumours with the help of bismuth-containing radiosensitisers.[42] In contrast, radionuclide therapy (internal radiotherapy) using radioactive bismuth nuclides is still in its infancy.[43,44] The increasing availability of the alpha-emitting nuclides ^{212}Bi and ^{213}Bi opens up a wide range of possibilities. This includes the use of radioactively labelled bifunctional chelating agents equipped with biological vector molecules and antibodies (BCFAs). There are new BFCAs with improved properties as well as selective and efficient coupling strategies, which opens up new opportunities for active targeting and the use of new radio-immunotherapeutic approaches. In addition, there is a rapid development in the field of bismuth-containing nanomaterials that are suitable for use in the combination therapy of cancer. This requires very defined particles in terms of size and morphology as well as the use of highly stable dispersions.

In this perspective article, suitable synthetic strategies for bismuth-containing materials will be discussed, which may allow a transfer to clinical use (Fig. 1). Furthermore, the state-of-the-art in the development of bismuth chelators for targeted alpha therapy is summarised and selected examples of radiolabelled target-seeking bioconjugates and nanomaterials are presented. New immunotherapeutic strategies are discussed that allow, on the one hand, effective recognition of tumours at an early stage and, on the other hand, various types of combination therapy for tumour treatment.

2. Bismuth materials: synthesis strategies and cancer applications

The synthesis of defined bismuth materials with high stability is difficult and challenging. In general, three classes of bismuth-containing materials can be distinguished, namely metallic nanoparticles (NPs), bismuth chalcogenides and bismuth-containing hybrid materials. With regard to clinical

Manja Kubeil

Manja Kubeil studied chemistry and received her Ph.D. degree from the Technische Universitat Dresden in 2014. In 2015, she was awarded with a Marie Curie International Outgoing Fellowship to undertake her post-doctoral research at the Monash University in Australia. In 2019, she became topic group leader at the Institute of Radiopharmaceutical Cancer Research at Helmholtz-Zentrum Dresden-Rossendorf (HZDR) in Germany. Since 2025, she is the head of Radiation Research on Biological Systems department at the Institute of Resource Ecology at HZDR. Her research focuses on radiopharmaceuticals for theranostic applications and radiation research to study the effects of radionuclides in living systems.

Michael Bachmann

Michael Bachmann Ph.D. in pharmacy (summa cum laude, Johannes-Gutenberg-University, Mainz, Germany), Professor of Physiological Chemistry, member of the Arthritis and Rheumatism Program (OMRF, OKC, U.S.A.), University Professor Medical Faculty (Technische Universität, Dresden, Germany), (i) tumour-immunology, (ii) Translational Radiopharmacology, and (Managing) Director, of the Institute of Radiopharmaceutical Cancer Research, at the Helmholtz Zentrum Dresden Rossendorf. Selected prizes: Boehringer-Ingelheim, Cell Biology, Bruno-Schuler (Rheumatology), Robert Feulgen (Int. Society of Cyto- and Histochemistry). Research focus: Radio-immunotheranostics for modular targeting systems (UniCAR, RevCAR, UniMAb). Current Research projects: Monash-Helmholtz Laboratory for Radio-Immuno-Theranostics (MHELTHERA), Ph.D. Networks: Oncoprotools, and Tolerate (European Union's Horizon Research and Innovation program).

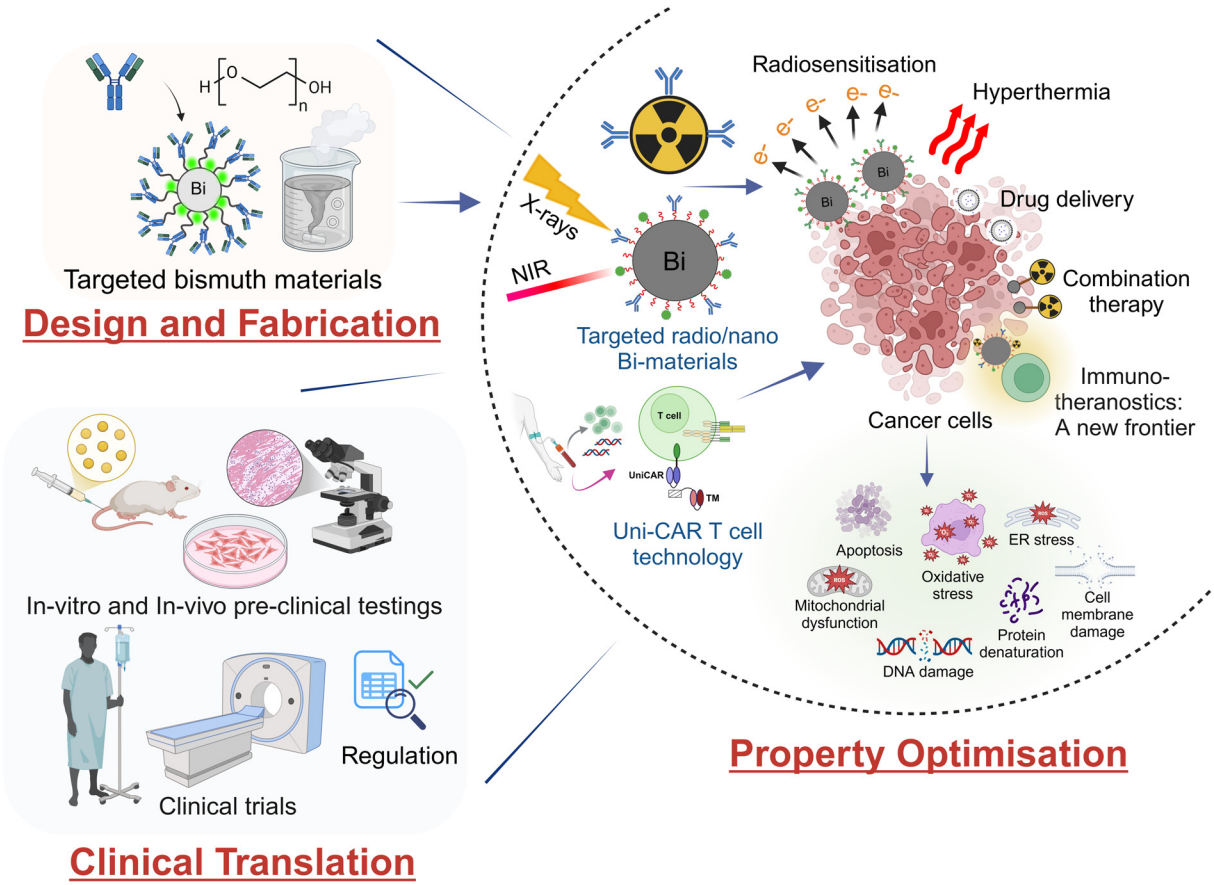

Fig. 1 Development and characterisation of bismuth materials for imaging and treating cancers with a view to clinical use.

use, materials with high biocompatibility and suitable surface functionalisation are required for biological targeting. In this perspective, the following chapter summarises various synthesis strategies for clinically relevant bismuth compounds and discusses selected examples of their use in cancer imaging and therapy.

Philip C. Andrews

Phil Andrews is the Head of the School of Chemistry at Monash University, Australia. After completing his PhD in 1992 at the University of Strathclyde, Glasgow, he held prestigious fellowships, including a Royal Society Fellowship at Griffith University and an Alexander von Humboldt Fellowship at Philipps Universität, Marburg. Joining Monash in 1995 he received an ARC QEII Fellowship, and is a Fellow of the Royal Society of Chemistry and the Royal Australian Chemical Institute. A founding member of the Monash Centre to Impact AMR, his research focuses on the discovery of metal compounds and materials as antimicrobials and anti-cancer agents.

Holger Stephan

Holger Stephan studied chemistry and received his PhD degree from the Technical University Bergakademie Freiberg in 1989. He held positions in industry and worked as Senior Scientist at the Technical University Dresden. In 1997, he moved to the Research Centre Rossendorf and was head of the working group "Nanoscalic Systems" at the Institute of Radiopharmaceutical Cancer Research of the Helmholtz-Zentrum Dresden-Rossendorf. He is currently working as the coordinator of the Monash-Helmholtz Laboratory for Radio-Immuno-Theranostics (MHELTHERA). His research focuses on the development of radiometal complexes, polynuclear metal compounds with photosensitizing and radiation-sensitizing properties, nanomaterials for multifunctional imaging and treatment of cancer.

2.1. Metallic bismuth nanoparticles

Owing to their unique properties, metallic bismuth particles have become very important.[45–48] The core characteristics of these particles are highly dependent on their crystal structure, size, shape and morphology, which can be tailored *via* various synthesis techniques.[49–51] These are essentially reduction methods, laser ablation, and thermal decomposition techniques. These methods can lead to particles with different size distributions and must be combined with suitable coating strategies for stabilisation in the complex biological environment.[52–54]

Synthesis strategies that use chemical reducing agents are the most commonly used methods for obtaining metallic bismuth materials. Reductive synthesis methods in the presence of stabilising molecules usually result in well-defined particles. For example, the reduction of $Bi(NO_3)_3$ using sodium borohydride in the presence of the biomacromolecules gelatin (GEL), bovine serum albumin (BSA) or human serum albumin (HSA) at 37 °C, was reported to form stable spherical particles with a narrow particle distribution, *i.e.*, the size range was 15.6 ± 3.1 nm for Bi@GEL, 17.4 ± 3.3 nm for Bi@BSA and 18.9 ± 3.8 nm for Bi@HSA, respectively.[55] Further, the cytotoxic anticancer drug doxorubicin (DOX) was incorporated, which allows for chemotherapeutic application. These biomacromolecule-stabilised metallic Bi-NPs have appropriate properties for theranostic applications, *i.e.*, they are suitable for CT and infrared thermal imaging (IRI) as well as for combination therapy based on chemo- and photothermal therapy.[55] Metallic Bi-NPs can also be stabilised with cellulose derivatives.[56,57] Chemical reduction using $NaBH_4$ yields very small particles (2–10 nm), while reduction using UV light results in larger particles 25–55 nm. The use of reducing bacterial cultures such as *Delftia* also enables the production of metallic Bi-NPs, albeit with relatively large particle sizes (40–120 nm).[58] Synthesis processes based on green chemistry are becoming increasingly important.[59,60] In this context, a promising way is to use biocompatible compounds as reducing agents. Ouyang *et al.* fabricated Bi-NPs from $BiCl_3$ using ethylene glycol as the reducing agent.[61] The metallic Bi-NPs obtained were coated with gold and doxorubicin was incorporated. These Bi@Au particles exhibit excellent blood compatibility, a high photoconversion efficiency (η = 46.6%) and are very effective in synergistic chemo-photothermal therapy proven in an A549 tumour-mice model. However, these particles are quite large at >100 nm. The use of viscous solvents like ethylene glycol slows the diffusion of reactants, which can lead to uneven nucleation and growth of particles.[62,63] There are a number of other Bi-NPs with sizes above 100 nm that exhibit good biocompatibility due to suitable surface functionalisation such as PEGylation, phospholipids and silica shells.[64,65] Smaller particles are better suited for biomedical applications, especially for clinical use.[66] One very interesting approach is the use of 45 nm-sized Bi-NPs, which have a SiO_2 shell for the incorporation of an H_2O_2-responsive prodrug.[67] These particles have very good photothermal properties with a high photoconversion efficiency (η = 46.3%) using near IR light at 808 nm. After intra-tumoural injection of these particles, photothermal ablation in combination with sequential X-ray irradiation allows for an improved therapeutic efficacy of >97%. Most of the Bi-containing particles currently used take advantage of passive targeting based on the enhanced permeability retention (EPR) effect.[68–70] The utilisation of active targeting with the help of biological vector molecules is only just beginning. In particular, specific peptides such as AR (androgen receptor) and LyP-1 as well as folate ligands are used for tumour targeting.[65,71–73] An interesting approach is to use the cancer cell membranes for targeting.[74]

To achieve ultrasmall particles, *i.e.* with sizes <6 nm, chemical reduction methods are also suitable if the appropriate reaction conditions are applied.[75,76] Lei *et al.* report a very fast (1 min) preparation method using $Bi(NO_3)_3$ as starting material, $NaBH_4$ and polyvinylpyrrolidone (PVP) as stabiliser, resulting in rapid generation of ultrasmall uniformly sized spherical Bi-NPs with a narrow size distribution (2.7 ± 1.1 nm).[75] It is worth mentioning that these Bi nanodots produce a higher CT contrast than the iodine-based contrast agent iobitridol. *In vivo* dual-modal CT/photothermal-imaging-guided therapy was demonstrated in a U14 tumour-mice model.[75] Similarly, very small Bi-NPs (3.6 nm) were obtained by reducing bismuth acetate in a mixture of oleic acid and oleylamine.[72] These primary particles were stabilised with a PEG and phospholipid shell and the nonapeptide LyP-1 is attached to the surface. The particles had a hydrodynamic diameter of 12 nm in aqueous solution and enabled dual imaging based on CT and PA. Moreover, a combination of NIR-laser and X-ray irradiation caused very effective tumour treatment (Fig. 2).

An elegant method of obtaining metallic particles is laser ablation, in which a high-intensity laser is used to generate NPs from a solid target.[77] Bulmahn *et al.* synthesized colloidal stable and pure Bi-NPs *via* femtosecond laser ablation of a metallic bismuth target. The results showed that metallic particles were only obtained in organic solvents like acetone, leading to spherical, primary Bi-NPs with narrow size distribution (28 ± 4 nm). In contrast, synthesis in water provides rather large nanosheets (455 ± 50 nm), consisting of bismuth subcarbonate. Colloidal stable aqueous solutions of metallic bismuth particles can be obtained in the presence of Pluronic® F68 as stabilising agent. However, DLS experiments show a broad particle distribution in the range of 50 to 150 nm. The metallic Bi-NPs showed efficient production of heat after irradiation with 808 nm NIR light, demonstrating their potential as promising photothermal agents for biomedical applications. Overall, laser ablation is a promising method for producing metallic bismuth particles, with the optimisation of various parameters such as laser energy, choice of solvent and stabilising compounds, allowing a wide range of particle size adjustment.[78]

The thermal decomposition of suitable bismuth compounds is another preparation route to produce metallic

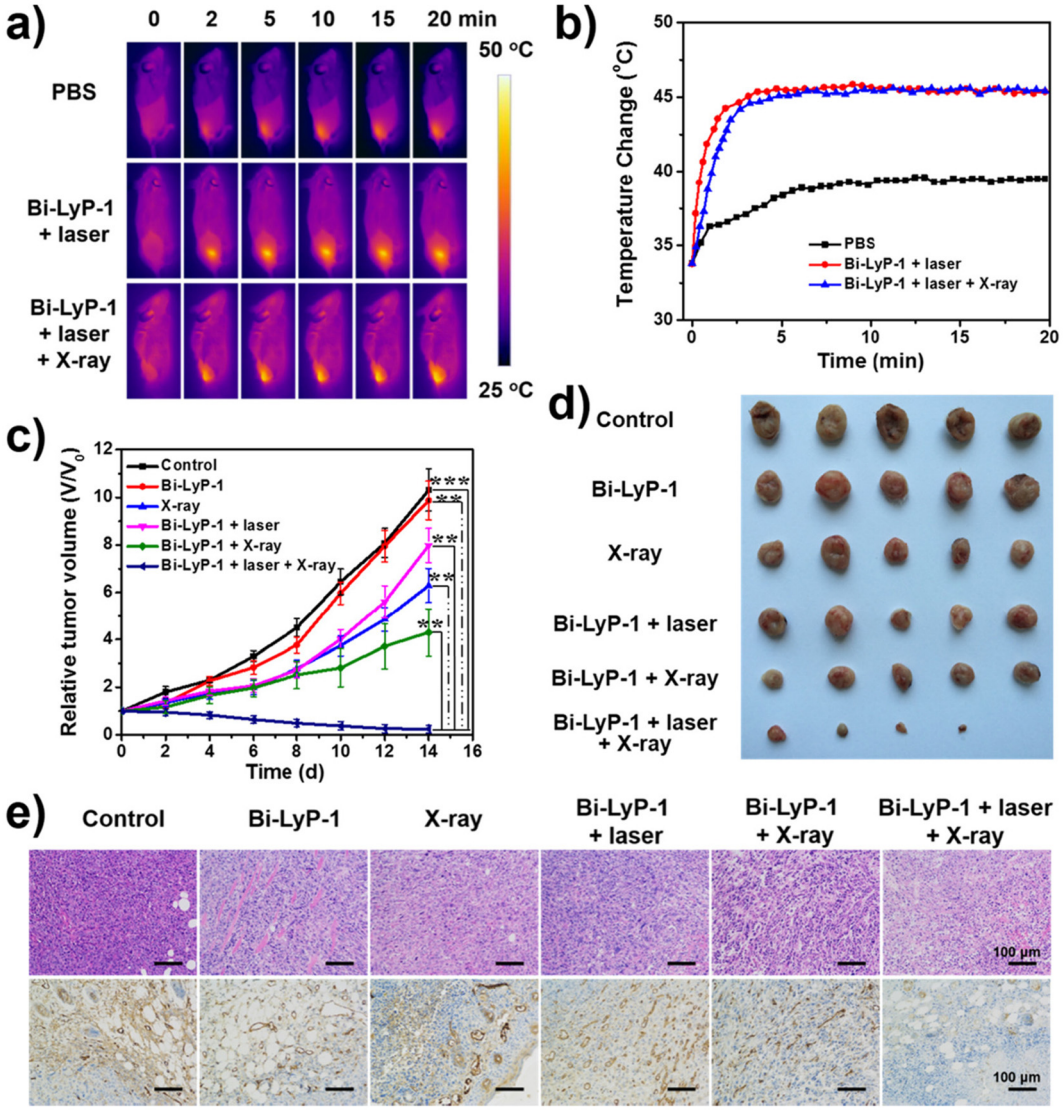

Fig. 2 Tumour treatment with Bi-NPs attached with the LyP-1 peptide (Bi-LyP-1 NPs). (a) IR images of 4T1 tumour bearing mice injected with Bi-LyP-1-NPs using 1064 nm laser irradiation (0.6 W cm^{-2}). (b) Temperature variation curves of tumour surface after NP's injection. (c) Tumour growth in each group under different treatments (d) Recorded images of tumour growth in different groups post 14 days. (e) H&E (upper row) and CD31 staining (bottom row) of tumour sections using different conditions (reprinted with permission from ref. 72, Copyright 2017 American Chemical Society).

Bi-NPs. It should be noted that reduction processes also occur simultaneously with the solvents used. The decomposition methods at high temperatures have several benefits, including precise control over NP size and shape by suitable temperature regimes, which allows for the adjustment of a well-defined crystal structure and fabrication of particles with narrow size distribution.[79] Thus, mono-dispersed spherical Bi-NPs (size ~ 4 nm) were obtained with high yield in a one-pot synthesis approach by using bismuth neodecanoate as precursor in octadecene/oleic acid solution at 260 °C.[79] These Bi-NPs can be stabilised with PEG-NH_2 in phosphate buffered solution, giving narrow-sized particles smaller than 10 nm. The Bi@PEG-NPs were biocompatible as demonstrated by their haemolytic tolerance and cell-viability assessment on L929 cells. Furthermore, these metallic particles show promising contrast (CT) and fluorescence properties that predestine them for *in vivo* imaging studies. Biodistribution experiments using ICP-MS analysis in BALB/c mice revealed accumulation in large intestine, liver, spleen and lungs accompanied by a rather slow clearance over 7 days. This behaviour is rather atypical for such ultrasmall particles and indicates a lack of stability *in vivo*.[80]

The table below summarises the composition of metallic bismuth nanoparticles, the corresponding manufacturing methods and conditions, as well as sizes, and provides an overview of possible applications in the imaging and therapy of cancers (Table 1).

Table 1 Summary of metallic Bi-NPs with varying surface functionalization, their synthesis methods and corresponding characterisation and applications

NPs composition	Synthesis method	System	Size [nm]	Application	Ref.
Bi@gelatin Bi@BSA Bi@HSA	Reduction	Bi nitrate $NaBH_4$ Doxorubicin	15.6 ± 3.1 17.4 ± 3.3 18.9 ± 3.8 (TEM)	CT/IRT imaging Chemo/PTT (tumour-bearing nude mice)	55
Bi@nanocellulose	Reduction	Bi nitrate $NaBH_4$ Nanocellulose-COOH	2–10 (TEM)	RT (4T1 tumour-bearing mice)	56
Bi@cellulose	Reduction	Bi/K citrate UV irrediation Carboxymethyl-cellulose Doxorubicin	25–55 (TEM/ DLS)	CT/PA imaging Chemo/PTT (4T1 tumour-bearing mice)	57
Bi@*delftia*	Reduction	Bi nitrate *Delftia* bacteria	40–120 (TEM)	*In vitro* cytotoxicity (HT29 cell line)	58
Bi@Au	Reduction	$BiCl_3$ Ethylene glycol Doxorubicin	>100 (DLS)	Chemo/PTT (A549 tumour-bearing mice)	61
Bi@PPy-PEG	Reduction	Bi nitrate Morpholine borane Polypyrrole (PPy)/PEG-dopamine coating	100–200 (TEM) 140–160 (DLS)	CT/PA imaging PTT (tumour-bearing BALB/c mice)	64
Bi@SiO_2	Reduction	Bi nitrate Dodecanethiol Silica coating Doxorubicin AR peptide	65 (TEM) 160–250 (DLS)	CT imaging Targeted chemo/PTT therapy (MCF-7 tumour-bearing mice)	65
Bi@SiO_2	Reduction	Bi dodecanethiolate Tri-octylphosphine Silica coating Redox-active prodrug	~25 (TEM) 45 (DLS)	IRT imaging PTT/RT (4T1 tumour-bearing mice)	67
Bi@Ag-PEG	Reduction	Bi nitrate Ag@PVP HS-PEG-folate Doxorubicine	>100 (TEM)	IRT imaging Chemo/PTT (A549 tumour-bearing mice)	71
Bi@DSPE-PEG	Reduction	Bi acetate Oleic acid Oleyl amine DSPE-PEG coating LyP-1 peptide	3.6 (TEM) 12 (DLS)	CT/PA imaging Targeted PTT/RT (4T1 tumour-bearing mice)	72
Bi@DSPE-PEG	Reduction	Bi nitrate Morpholine borane PEG2000-DSPE-folate coating	40 (TEM) 56 (DLS)	Targeted RT (4T1 tumour-bearing mice)	73
Bi@DSPE-PEG	Reduction	Bi dodecanethiolate Oleyl amine Octadecene CT26 cancer cell membrane-coating	42 ± 2 (TEM)	Targeted PTT (CT26 tumour-bearing mice)	74
Bi@PVP	Reduction	Bi nitrate $NaBH_4$ PVP	2.7 ± 1.1 (TEM) 10.8 (DLS)	CT/IRT imaging PTT (U14 tumour-bearing mice)	75
Bi@DLPC	Reduction	Bi acetate Dodedanethiol Oleic acid Trioctylphospine DLPC coating	47 ± 3 (TEM) 162 (DLS)	CT/PA imaging PTT (MDA-MB 231 tumour-bearing mice)	81
Bi@RBC	Reduction	Bi nitrate HNO_3 PVP $NaBH_4$ RBC membrane vesicles DSPE-PEG_{2000}	196 ± 4 (DLS)	RT/PTT (LLC tumour bearing mice)	82
Bi@Pluronic®F68	Laser ablation	Bi target in acetone	28 ± 4 (TEM) 50–150 (DLS)	Photothermal properties	77
Bi@PEG-NH_2	Thermal decomposition	Bi-neodecanate Octadecene Oleic acid	4 (TEM) <10 (DLS)	CT/fluorescence imaging Biodistribution in BALB/c mice	79

BSA, bovine serum albumin; CT, computed tomography imaging; DLPC, 1,2-dilauroyl-*sn-glycero*-3-phosphocholine; DOX, doxorubicin; DSPE, 1,2-distearoyl-*sn-glycero*-3-phosphoethanolamine; HSA, human serum albumin; IRT, infrared thermography; PA, photoacoustic imaging; PEG, polyethylene glycol; Pluronic®F68, polyoxyethylene/polyoxypropylene block copolymer; PTT, photothermal therapy; RBC, red blood cell; TGA, thioglycolic acid; UV, ultraviolet.

2.2. Bismuth chalcogenides

Bismuth chalcogenides (Bi_2X_3) constitute unique layered structures composed of bismuth (Bi) with chalcogen elements (X) such as sulfur (S), oxygen (O), selenium (Se), or tellurium (Te).[83] It represents a class of materials, which are generally non-toxic in nature, inexpensive and highly stable.[84] Due to their diverse features such as unique optical, thermal and electronic properties,[85,86] bismuth chalcogenides have been exploited for a variety of applications like thermo-responsive electronics, photovoltaics, (bio)catalysis, sensing as well as cancer imaging and therapy.[83,87–89] With regard to the latter, bismuth chalcogenides combine their structural diversity with a high degree of biocompatibility, efficient light-to-heat conversion in the NIR region and radio-enhancement abilities, leading to exceptional image-guided dual theranostic modalities.[34,90,91] Moreover, suitable surface functionalisation and the introduction of biological vector molecules can lead to improved biocompatibility and increased tumour targeting, making them interesting for a wide range of biomedical applications.[91,92]

Hydrothermal methods are the most frequently used processes for producing stable Bi_2X_3 nanomaterials. In this process, bismuth precursors are reacted with chalcogen-containing compounds in an aqueous medium at elevated temperatures and suitable pressure. Depending on the conditions used, different sizes and shapes are obtained. Bi_2S_3-NPs are the most frequently pre-clinical studied bismuth chalcogenides in the imaging and therapy of cancers. A few selected examples are discussed below. The reaction of Bi_2O_3 precursors with thioacetamide (TAA) under pressure at elevated temperature and subsequent PEGylation leads to rather large, colloidal stable particles (>200 nm), which can be loaded with 3-bromopyruvate for enhanced radiosensitising. The resulting particles were shown to serve as efficient bimodal contrast agents for CT/PA imaging and demonstrate excellent X-ray sensitisation and NIR optical absorption properties, leading to high therapeutic efficacy against 4T1 breast tumours.[93] An interesting approach is described by Poudel *et al.*, which results in larger particles (173.5 ± 2.8 nm). Starting from Bi_2O_3 nanoshells, a hydrothermal synthesis under pressure in the presence of TAA is used to convert them into Bi_2S_3-based 'nano-urchins', which are loaded with indocyanine green (ICG). PEGylation is used for colloidal stabilisation and to introduce the anticancer drug methotrexate and folate units for targeting. In this way redox and photo-responsive targeted Bi_2S_3-NPs can be produced for simultaneous use in chemotherapy, PDT and PTT.[94] Bi_2S_3 nanorods (60 × 130 nm) were produced by hydrothermal synthesis and stabilised in an aqueous environment using PVP. These particles were then coated with mesoporous silica, loaded with doxorubicin and equipped with the antibody trastuzumab for targeting. The nanorods have excellent contrast and photothermal properties and enable the application of targeted, effective cancer therapy based on chemo- and PTT.[95] Overall, colloidally stabilised Bi_2S_3-NPs of this size are subject to the problem of a long residence time in the body.

Bi_2O_3, Bi_2Se_3 and Bi_2Te_3-NPs are also accessible *via* hydrothermal routes and exhibit interesting photothermal and radiosensitising properties.[96,97] 80 nm-sized Bi_2O_3-NPs are obtained by hydrothermal synthesis in the presence of Triton X and chitosan as a coating agent. These particles are loaded with the photosensitiser 5-aminolevulinic acid (5-ALA) and the anticancer agent curcumin. These particles can be used for CT imaging. Initial investigations into the therapeutic efficacy of chemotherapy and radiotherapy show effects, but these still need to be optimised.[91] Very small 6 nm-sized bismuth ferrite NPs were synthesised *via* a facile hydrothermal method. After coating with poly(acrylic acid), these particles can be applied for PTT/PDT combination therapy.[98] An elegant method that, in the presence of selenocysteine, leads to well-defined, 15 nm-sized Bi_2Se_3-NPs, is described by Du *et al.*[99] These selenocysteine-modified NPs coated with PVP are highly biocompatible and show high therapeutic efficacy *in vivo* when radiotherapy and PTT are used simultaneously. It is worth mentioning that selenium can enter the bloodstream in parts and stimulate the immune system, as well as achieve a radioprotective effect throughout the body (Fig. 3).

The production of bismuth chalcogenides in organic solvents (solvothermal synthesis) instead of water usually results in smaller particles. Various shapes are available in this way. Bi_2S_3 nanorods,[90,100–104] Bi_2S_3 nanosheets,[105] Bi_2O_3 spherical particles,[106,107] Bi_2Te_3 nanosheets[108] and Bi_2Te_3 spherical particles[109] have been generated using the solvothermal technique. The so-called polyol process yields relatively small homogeneous particles, for example Bi_2O_3 (40–50 nm), which can be stabilised with hyaluronic acid.[110] These particles exhibit excellent contrast and radiosensitising properties and are being discussed for use in CT imaging-guided radiotherapy. Small Bi_2O_3-NPs (19.2 ± 6.5 nm) were produced in propylene glycol and then coated with a silica shell, which has terminal NH_2 groups for conjugation of folic acid and the photosensitiser 5-ALA. These particles show high *in vitro* cell toxicity after UV irradiation and are being discussed for use in PDT.[106] Silica-coated 100 nm large Bi_2S_3-NPs were produced *via* a surfactant-assisted solvothermal synthesis.[111] The NPs were loaded with doxorubicin and RGD peptides were incorporated as biological vector molecules using a PEG linker. These particles can be used for dual imaging (CT/IRT) and show a high therapeutic efficacy based on combined chemotherapy and PTT. Bi_2S_3 nanorods were prepared in organic solution, then coated with a thermally retracted poly(acrylamide) based polymer, where the photosensitiser zinc protoporphyrin X has been linked. This system shows promising contrast (CT), photodynamic and photothermal properties, enabling the combination of PDT and PTT.[104] Oleyl amine-capped 36 nm-sized Bi_2Te_3-NPs have been fabricated, stabilised in biological environment by phospholipid-PEG coating and then loaded with a Pt(IV) prodrug. These particles show a very high photoconversion efficiency (η = 48.7%), are suitable for dual imaging (PA/IRI) and enable effective combination therapy based on

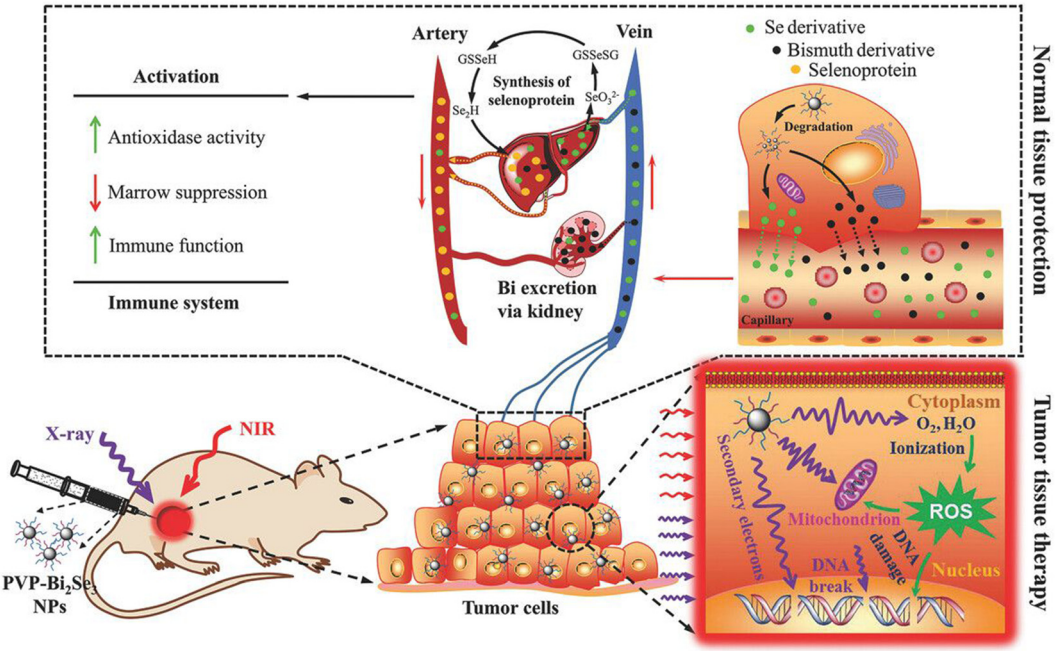

Fig. 3 Schematic illustration of the therapeutic principle based on Bi_2Se_3@PVP nanoparticles, containing selenocystein (Sec) for simultaneously synergistic photothermal/radiotherapy of tumour and enhancement of the immunity to reduce the side effects of radiation. (Reprinted with permission from ref. 99, Copyright 2017, WILEY-VCH Verlag GmbH & Co.)

chemotherapy and PTT.[109] Chen *et al.* report on an immunotherapeutic approach using sulphur-doped Bi_2O_3-NPs, which were produced in ethylene glycol and then stabilised with PVP.[112] These NPs are loaded with the drug Ivermectin and induce a highly effective immunogenic cell death of tumours by combining PTT and a sonocatalytic therapy. Bi_2Se_3-NPs are also obtained by solvothermal synthesis and stabilised using PVP.[113] These particles are then coated with polydopamine, loaded with doxorubicin and stabilised with HSA. These particles can be used for dual imaging (CT/IRT) and show a synergistic therapeutic effect when PTT and chemotherapy are applied in a tumour mouse model.

Over the last 10 years, biomineralisation methods have been used to produce bismuth chalcogenides. This method has been reported to generate Bi_2S_3 spherical particles with sizes generally below 50 nm, possessing good stability in complex biological environment and high biocompatibility.[114–122,123] The treatment of bismuth precursors in the presence of BSA leads to defined Bi_2S_3-NPs and was first described by Wang *et al.* in 2016.[120] The primary particles are smaller than 10 nm (TEM). However, DLS measurements show a size of around 40 nm. Accordingly, the accumulation of Bi_2S_3-NPs occurs not only in the tumour but also in the liver, spleen, kidneys and lungs, as shown by biodistribution studies with ^{99}Tc-labelled particles. These particles are suitable for imaging based on CT and IRT. *In vivo* studies in a tumour mouse model show that a combination of radiotherapy and PTT can achieve complete tumour remission. In terms of a therapeutic application, BSA-stabilised Bi_2S_3-NPs are mainly used in radio-, chemo- and immunotherapy, or a combination of these.[114,122,124,125] Curcumin, specific peptides such as triptorelin, folic acid and the immunoactive ganoderma lucidum polysaccharide (GLP) are used to increase the effectiveness of the therapy and for targeting. While the primary particles Bi_2S_3@BSA are rather small, with sizes around 10 nm, larger associates of around 100 nm are often found in the biological environment. An interesting approach for *in vivo* applications is the use of 3D-printed alginate scaffolds with Bi_2S_3@BSA-NPs.[123] These implanted scaffolds show a high therapeutic efficacy in a tumour mouse model after X-ray irradiation and are discussed for post-surgical use to remove residual tumour cells in breast cancer patients. Ultrasmall Bi_2Se_3-NPs (3 nm) were obtained by biomineralisation and encapsulated in tumour cell-derived microparticles together with doxorubicin.[126] These particles are ideal for image-guided tumour targeting with subsequent combination of chemotherapy and PTT.

The table below summarises the composition of bismuth chalcogenide-based nanoparticles, the corresponding manufacturing methods and conditions, as well as sizes, and provides an overview of possible applications in the imaging and therapy of cancers (Table 2).

2.3. Bismuth hybrid materials and nanocomposites

Bismuth-based hybrid materials and nanocomposites that consist of other inorganic or organic compounds and are equipped with target-seeking units are becoming increasingly important. Bismuth and bismuth compounds, when com-

Table 2 Summary of Bi_2X_3-NPs with varying surface functionalization, their synthesis methods and corresponding characterisation and applications

NPs composition	Synthesis method	System	Size [nm]	Application	Ref.
Bi_2O_3@Chitosan	Hydrothermal	Bi nitrate Triton-X Chitosan 5-ALA and curcumin loading	80 (TEM) 204 (DLS)	CT imaging Chemo/RT (4T1 tumour bearing mice)	91
Bi_2S_3@PEG-SH	Hydrothermal	Bi_2O_3 Thioacetamide PEG-SH coating 3-Bromopyruvate loading	260 (DLS)	CT/PA imaging RT (4T1 tumour-bearing mice)	93
Bi_2S_3@(ICG)-PEG-S-S-MTX	Hydrothermal	Bi_2O_3 nanoshells Thioacetamide ICG loading SH-PEG-S-S-MTX	173.5 ± 2.8 (DLS)	Targeted Chemo/PTT/PDT (HCT116 tumour bearing mice)	94
Bi_2S_3@PVP(SiO_2)	Hydrothermal	Bi nitrate Ethylene glycol Sodium sulfide PVP (SiO_2) Trastuzumab DOX loading	Diameter 26 Length 100 (TEM)	CT imaging Targeted Chemo/PTT (SKBR-3 tumour bearing mice)	95
Bi_2O_3@Fe-PAA	Hydrothermal	Bi nitrate Fe nitrate Poly(acrylic acid)	6 (TEM) 69.6 ± 1.6 (DLS)	PTT/PDT (HepG2 tumour-bearing mice)	98
Bi_2Se_3@PVP	Hydrothermal	Bi nitrate PVP L-Selenocystine	15 ± 3 (TEM) 29.2 (DLS)	PTT RT (Bel-7402 tumour-bearing mice)	99
Bi_2S_3@PAA	Solvothermal	Bi neodecanoate Thioacetamide Oleic acid Oleyl amine PAA coating Protoporphyrin IX	∅ 13 ± 2 l = 40 ± 5 (TEM)	CT/IRT imaging PTT/PDT therapy (4T1 tumour bearing mice)	104
Bi_2O_3@SiO_2-NH_2	Solvothermal	Bi nitrate Propylene glycol APTMS functionalization 5-ALA and folic acid conjugation	19.2 ± 6.5 (TEM)	PDT (KB cell line)	106
Bi_2Te_3@DSPE-PEG	Solvothermal	Bi neodecanoate TrioctylP-Te DSPE-PEG-CH_3 coating Pt(IV) prodrug loading	36 (TEM)	PA/IRT imaging Chemo/PTT (4T1 tumour bearing mice)	109
Bi_2O_3@HA	Solvothermal	Bi chloride NaOH Diethylene glycol Hyaluronic acid	45 ± 0.6 (TEM) 47.4 (DLS)	CT imaging RT (tumour bearing mice)	110
Bi_2S_3@SiO_2-NH_2	Solvothermal	Bi chloride Na_2S Ethylene glycol CTAC APTES DOX loading RGD peptide	100 (TEM) 120 (DLS)	CT/IRT imaging Targeted Chemo/PTT (UMR-106 tumour bearing mice)	111
$Bi_2O_{3-x}S_x$@PVP	Solvothermal	Bi nitrate Ethylene glycol NH_4F, Na_2S PVP Ivermectin	30 (TEM) 130 (DLS)	PTT Sonocatalytic therapy (4T1 Balb/c female mice)	112
Bi_2Se_3@PDA	Solvothermal	Bi nitrate Na_2SeO_3 Ethylene glycol PVP, PDA DOX loading HSA	104 (TEM) > 400 (DLS)	CT/IRT imaging Chemo/PTT (HeLa tumour bearing mice)	113

Table 2 *(Contd.)*

NPs composition	Synthesis method	System	Size [nm]	Application	Ref.
Bi_2S_3@BSA	Biomineralisation	Bi nitrate BSA FA coupling Curcumin loading FITC labeling	<10 (TEM) 170 (DLS)	CT imaging RT (4T1 tumour bearing mice)	114
Bi_2S_3@BSA	Biomineralisation	Bi nitrate BSA HNO_3 NaOH	6.1 ± 0.9 (TEM) 40 (DLS)	CT/IRT imaging PTT/RT (4T1 tumour bearing mice)	120
Bi_2S_3@BSA	Biomineralisation	Bi nitrate HNO_3 NaOH BSA Curcumin	15 ± 4 (TEM) 100 (DLS)	*In vitro* Chemo/RT (HT-29 cells)	122
Bi_2S_3@BSA	Biomineralisation	Bi nitrate BSA Triptorelin	8.5 ± 1.5 (TEM) 17 ± 2 (DLS)	*In vitro* RT (MCF-7 cells)	124
Bi_2S_3@BSA	Biomineralisation	Bi nitrate HNO_3 NaOH BSA GLP-SH	10 ± 3 (TEM) >130 (DLS)	RT/immuotherapy (4T1 tumour-bearing BALB/c mice)	125
Bi_2S_3@BSA	Biomineralisation	Bi nitrate BSA Alginate	21.6 ± 5.7 (TEM) 55 (DLS)	RT (4T1 tumour bearing mice)	123
Bi_2Se_3@BSA	Biomineralisation	Bismuth chloride Selenium powder Ethylenediamine Mercaptoethanol BSA Doxorubicin H22 tumour cell-derived microparticles	3.0 ± 0.4 (TEM) 13.5 ± 1.5 (DLS)	CT/PA imaging Targeted Chemo/PTT (H22-tumour-bearing mice)	126

5-ALA, 5-aminolevulinic acid; APTES, 3-aminopropyltriethoxysilane; BFO, bismuth ferrite; BSA, bovine serum albumin; CT, computed tomography imaging; CTAB, cetyltrimethylammonium bromide; Cur, curcumin; DOX, doxorubicin; FA, folic acid; GLP, ganoderma lucidum polysaccharide; HSA, human serum albumin; ICG, indocyanine green; IRT, infrared thermography; mPS, mesoporous silica; MTX, methotrexate; PA, photoacoustic imaging; PDA, polydopamine; PDT, photodynamic therapy; PEG, polyethylene glycol; PM, platelet membrane; Pt, platinum; PTT, photothermal therapy; TEOS, tetraethyl orthosilicate; US, ultrasound.

bined with other metals and metal compounds, organic materials such as stimuli-response polymers or carbon-based structures, provide novel functionalities and improved performances due to the synergistic interplay of the components, rendering nanohybrids/nanocomposites novel versatile functionalities.[127–129] In the field of cancer research, on the one hand improved contrast properties can be achieved in imaging, while on the other, the range of treatment options for cancer can be expanded. Concerning the latter, emerging technologies for optimisation of targeted PTT, PDT, RT, hypoxia modulation, and combinatorial therapeutic regimes are in a state of rapid development.[130–132]

In the following, there are a few examples that show the diversity in this field and provide an insight into new fields of application. The combination of bismuth in its metallic form or various bismuth chalcogenides with metals such as Ag, Au, Pt and Pd leads in particular to improved contrast and radiosensitising properties, harnessing narrow band gaps and enables the use of highly effective sonodynamic therapy.[133–137] By mixing bismuth chalcogenides with metallic Bi-NPs, the bismuth content can be increased compared to the chalcogenides alone, thus significantly boosting both the contrast properties and the effectiveness of PTT.[138–141] Bismuth molybdate- and tungstate-based nanomaterials are gaining importance as sonosensitisers.[142,143] Polyoxometalates (POMs) are an extremely interesting class of substances for cancer therapy.[144,145] POMs have the great advantage that they can be produced in a very defined manner over a wide size range. However, the surface functionalisation is not trivial. Due to their radiosensitising properties, bismuth-containing POMs are of interest for improving the effectiveness of RT.[146] New drug delivery systems based on biocompatible bismuth-containing metal–organic frameworks (MOFs) should also be mentioned.[147] This field of research is only just beginning. However, it offers a wide range of biomedical applications. The blending of bismuth-containing materials with graphene oxide (GO) and reduced graphene oxide (rGO) is used to improve biocompatibility and for drug delivery. In addition, GO/rGO can be used to adjust the electrical and thermal conductivity of hybrid materials very precisely, thus enhancing imaging and

radiosensitisation properties.[127,148–151] In recent years, considerable work has been done on the development of hybrid materials with the addition of manganese oxide, magnetite and gadolinium oxide.[116,152–158] This provides magnetic resonance tomography (MRT) as an additional imaging technique that is particularly suitable for good soft tissue contrast. With respect to its use in cancer therapy, the efficacy of hyperthermia can be increased and a hypoxia-related radioresistance can be overcome with these materials. An interesting inorganic–organic hybrid material is described by Zhang *et al.* in which metallic Bi-NPs are coated with silica and then stabilised with an organic polymer to which porphyrin loaded with iron(II) is covalently bound.[159] This material can be used for combination therapy consisting of chemotherapy, PTT and PDT. Core–shell nanocomposites, consisting of ultra-small Bi_2S_3 nanoparticles, cerium oxide and the photosensitiser chlorin e6 have been developed for NIR-triggered PDT.[160] Liu *et al.* reported a biodegradable and biocompatible core–shell bismuth-based hybrid material coated with a MnO_2 layer and loaded with the anticancer drug docetaxel (DTX) to treat radioresistant hypoxic tumours. The bismuth/manganese-based radiosensitising material has been stabilised with amphiphilic PEG equipped with folic acid as target-seeking groups (Fig. 4). For this targeted nanocomposite, an efficient CT/MR image-guided combination therapy based on chemotherapy, chemodynamic therapy and radiotherapy is described for a tumour mouse model.[155]

3. Radiolabelled bismuth compounds

Radiolabelled compounds enable both imaging and the treatment of cancer. Bismuth offers two isotopes of interest for radiopharmaceutical applications. Both of them partially emit α-particles and decay *via* short-living daughter nuclides, which is expected to limit off-target accumulation.[161] One promising candidate for targeted alpha therapy (TAT) is ^{212}Bi, which decays *via* a branched pathway to ^{208}Tl ($t_{1/2}$ = 3.1 min, 36% α) and ^{212}Po ($t_{1/2}$ = 0.3 μs, 64% β^-) and finally to stable ^{208}Pb. It can be eluted from a ^{224}Ra/^{212}Pb/^{212}Bi generator system as $[^{212}Bi][BiI_5]^{2-}$/$[^{212}Bi][BiI_4]^-$, either selectively or co-eluted with ^{212}Pb. Due to the short half-life of ^{212}Bi ($t_{1/2}$ = 60.55 min), co-elution and subsequent use as a ^{212}Pb/^{212}Bi *in vivo* generator became of interest over the last few years.[162,163] However, one major issue is the high energetic γ-line emitted by ^{208}Tl (E_γ = 2.6 MeV), which can be problematic regarding dosimetry.[164]

The second isotope of interest is ^{213}Bi ($t_{1/2}$ = 45.6 min), one longer living daughter nuclide of ^{225}Ac. It decays *via* ^{209}Tl ($t_{1/2}$ = 2.2 min, 2% alpha) and ^{213}Po ($t_{1/2}$ = 3.7 μs, 98% beta) to ^{209}Pb ($t_{1/2}$ = 3.2 h) and ultimately to ^{209}Bi (stable). It can be eluted from the respective ^{225}Ac/^{213}Bi generator as $[^{213}Bi][BiI_5]^{2-}$/$[^{213}Bi][BiI_4]^-$, but the separation from the other daughter nuclides ^{221}Fr ($t_{1/2}$ = 4.9 min) and ^{217}At ($t_{1/2}$ = 32.3 ms) can be challenging. A mixture of 0.1 M HCl/0.1 M HI was found to enable selective elution of ^{213}Bi.[164]

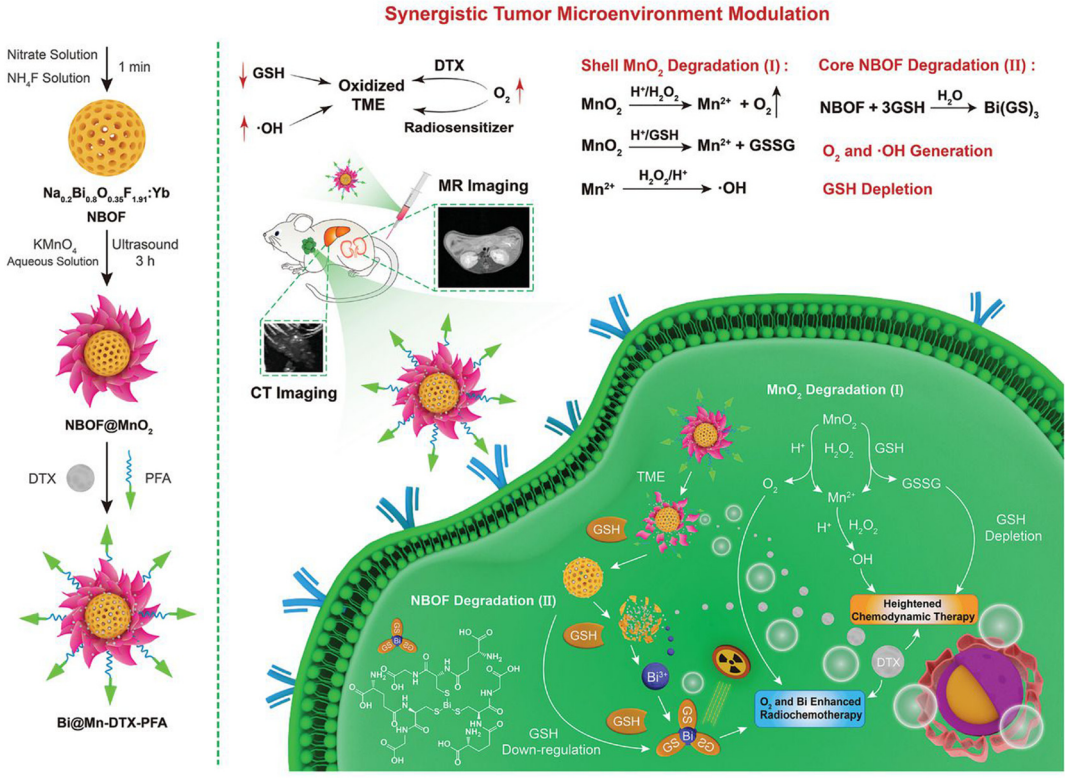

Fig. 4 Schematic diagram of the synthesis process of Bi@Mn-DTX-PFA and its synergistic therapy mechanism for hypoxic tumours. (Reprinted with permission from ref. 155, Copyright 2021 John Wiley and Sons.)

The relatively short half-life of $^{212/213}$Bi can be advantageous for radiopharmaceutical applications, but some studies (*e.g.* biodistribution studies) can require measurements over a longer time. For that purpose, the β^+-emitter $^{205/206}$Bi ($t_{1/2}$ = 14.9 d and 6.2 d) can be used instead. While ^{206}Bi decays directly to stable ^{206}Pb, ^{205}Bi decays *via* the long living daughter ^{205}Pb ($t_{1/2} = 1.7 \times 10^7$ years) to stable ^{205}Tl.[165–167] $^{205/206}$Bi can be obtained by irradiation of ^{nat}Pb with a proton beam for up to 7 h and selectively eluted from a Pb-SpecTM resin (18-crown-6-based resin) using HNO_3.[168]

To ensure safe delivery of bismuth radioisotopes to the targeted tissue, a wide range of chelators (Scheme 1) have been developed with some already tested *in vivo*. One class of interest is acyclic chelators, which typically enable fast labelling kinetics under mild conditions. Prominent examples are DTPA (diethylenetriaminepentaacetic acid) and its derivatives, which were conjugated to a variety of proteins.[40,169,170] However, some of the derivatives were found to be unstable, which led to the development of CHX-A″-DTPA, in which a cyclohexyl moiety was installed in the backbone to provide rigidity and improve the stability.[170] Other promising acyclic chelators such as H_4Neunpa and H_2ampa showed favourable labelling kinetics, high molar activities and provided high stabilities (pM = 26 for $[Bi(ampa)]^+$).[161,171]

Cyclic chelators generally form highly stable complexes, but the formation kinetics of the respective complex can be slow. The gold standard for a broad range of metals is DOTA (1,4,7,10-tetraazacyclododecane-1,4,7,10-tetraacetic acid), a cyclen-based chelator that undergoes continuous optimization to match the chemical requirements of different metals even better. The introduction of "soft" electron donors such as phosphonic acids was found to increase the thermodynamic stability of the complex and lead to higher radiolabelling efficiencies compared to the carboxylic acid bearing DOTA.[172]

Another subclass is based on the crown ether macropa (*N*,*N*′-bis((6-carboxy-2-pyridil)methyl)-4,13-diaza-18-crown-6), which is also known to form stable complexes and, in contrast to DOTA, forms complexes at milder reaction conditions. Especially py-macrodipa, a derivative with one oxygen donor replaced by a nitrogen and a pyridine ring attached to the backbone, showed efficient radiolabelling with ^{213}Bi after 5 min at room temperature.[173] Recently, it was shown that the introduction of sulphur donors into the macropa system reduces both the thermodynamic stability and the kinetic inertness of (radio)bismuth complexes.[174]

Characteristics of both chelator classes are combined in bispidines (3,7-diazabicylco[3.3.1]nonanes), which have a rigid backbone but flexible side arms to form stable complexes under mild conditions. Some octa- and nonadentate bispidines (L^1–L^5) were investigated and especially the nonadentate ones were found to be promising candidates for TAT.[175,176]

3.1 Radiolabelled small molecules, peptides and proteins

Targeted radiobismuth therapies have been applied with small molecules, peptides, antibody fragments, monoclonal antibodies, or any other kind of immunoproteins. They have shown promising results in pre-clinical and clinical studies in various tumour entities especially in small-volume or micrometastasis such as breast cancer,[177–179] bladder cancer,[180]

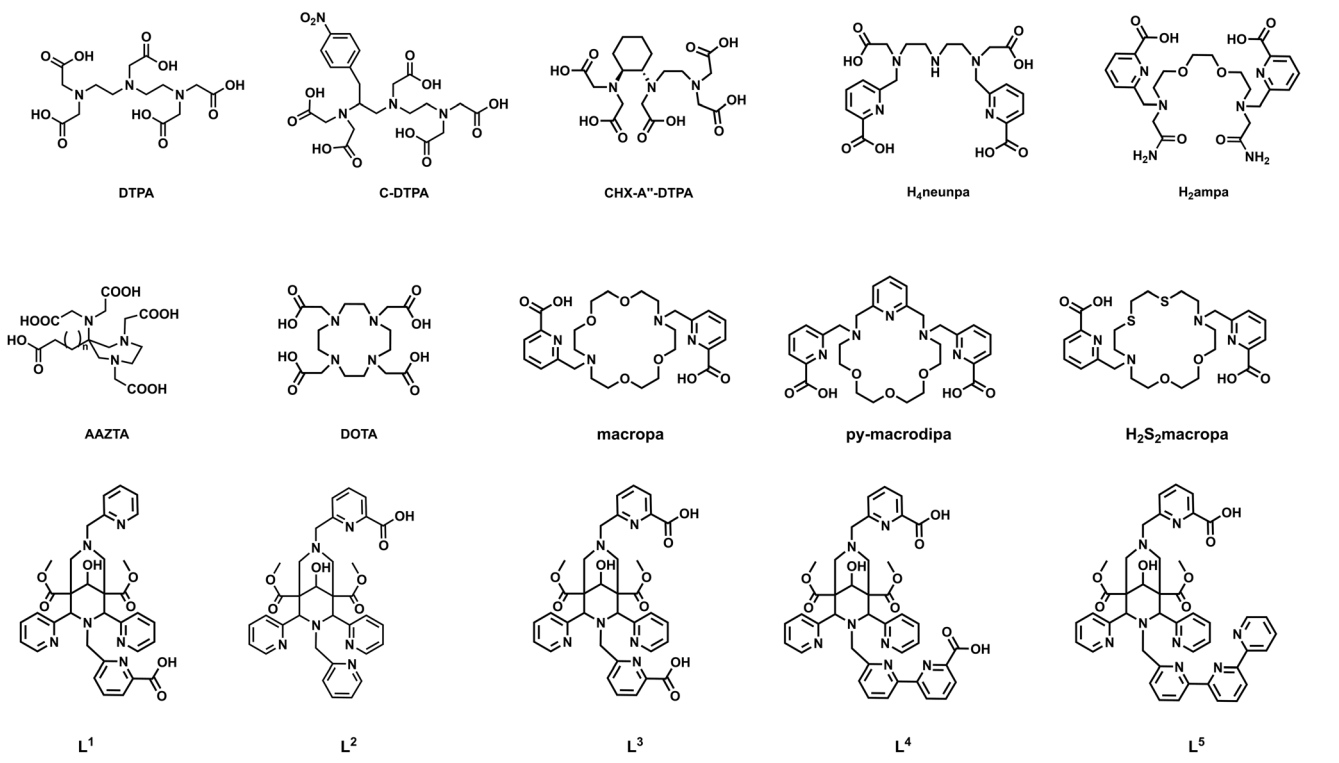

Scheme 1 Chemical structures of acyclic and macrocyclic chelators for bismuth(III) discussed in this article.

colon cancer,[181,182] glioma,[183,184] melanoma,[165,171,185–188] multiple myeloma,[189–191] non-Hodgkin lymphoma,[192,193] ovarian cancer,[194–196] pancreatic cancer and neuroendocrine tumours[197–202] and prostate cancer.[203] Of note, the first radiobismuth immunoconjugate (^{212}Bi-CHIP) was studied in human pancreatic carcinoma cells (SHAW) in 1988.[200] To this end, the results are summarized in other reviews,[40,169,170] in which TAT showed success with locoregional and systemic administration. Herein, we only focus on recently published pre-clinical studies and highlight the clinical translations of radiolabelled bismuth conjugates.

3.1.1 Bladder cancer. In a recent pilot bacillus Calmette Guèrin (BCG) therapy study, 12 patients with carcinoma *in situ* (CIS) were treated with [^{213}Bi]Bi-CHX-A″-DTPA-anti-EGFR-mAb by injecting 366–821 MBq *via* transurethral catheter. The pilot study proved that no severe side effects were observed in all patients. However, the authors addressed several strategies to improve therapeutic efficacy (3 out of 12 patients showed complete eradication after treatment).[169]

3.1.2 Glioma. In an initial study, five patients with critically located gliomas were treated with the neurokinin type-1-receptor (NK-1) targeting conjugate [^{213}Bi]Bi-DOTA-SP (substance P). Substance P, a small peptide with a weight of 1.8 kDa, showed high NK-1 affinity in the nanomolar range, which in turn was found to be selectively overexpressed in all malignant glioblastomas. Biodistribution studies were performed by co-injection of the ^{68}Ga-labelled conjugate *via* an intratumoural catheter. One patient received 7.36 GBq of the conjugate over 4 therapeutic cycles, the rest was treated in one cycle with 1.07–2.00 GBq of [^{213}Bi]Bi-DOTA-SP. All patients showed radionecrotic effects on the tumour, however the patient with the lowest dose administered showed only 50% reduction in tumour volume. No severe local or systemic toxicity was observed in any of the patients.[204]

A subsequent study with 50 patients was performed with [^{213}Bi]Bi-DOTA-SP, where nine patients were diagnosed with secondary glioblastomas and the rest with different types of malignant gliomas. The median total dose administered over 1–6 cycles was 5.8 GBq and ranged between 1.4–9.7 GBq. The overall survival of patients who received [^{213}Bi]Bi-DOTA-SP was extended to ten months in comparison to patients who underwent surgical resection only (overall survival of two months).[205]

In the latest glioma study, 20 patients with recurrent glioblastoma were treated with [^{213}Bi]Bi-DOTA-SP (substance P) with a median injected activity of 3.3 GBq in total. The median overall survival of treated patients increased to 10.9 months after diagnosis of recurrence.[183]

3.1.3 Melanoma. For metastatic uveal melanoma, [^{213}Bi](BiNeunpa-Ph-Pip-Nle-CycMSH$_{hex}$) targeting melanocortin 1 receptor (MC1R) was studied *in vivo*. Labelling of the conjugate was performed at room temperature at pH 5, achieving molar activities up to 21 MBq nmol^{-1} after 5 min of incubation. The novel bismuth complex showed high stability (pM = 27.0) as well as high chemical inertness in human serum over 2 h. The conjugate showed high tumour uptake in B16-F10 tumour xenografted mice (5.91 %ID g^{-1} 1 h p.i.).[171]

The biodistribution of [$^{205/206}$Bi]Bi-DOTA-IPB-NAPamide in B16-F10 tumour bearing mice was investigated with and without the albumin binder 4-(*p*-iodo-phenyl)butyryl (IPB) to prolong the circulation time and therefore increase the tumour uptake. Higher tumour uptake was observed for the IPB containing conjugate (4.50 %ID g^{-1} *vs.* 3.14 %ID g^{-1}), but high off-target accumulation in kidneys (8.78 %ID g^{-1}) as well. Therefore, application of albumin binders for short-living radionuclides was found to be disadvantageous.[165]

In a first initial patient trial the efficacy of a radiobismuth labelled monoclonal antibody targeting melanoma receptors (melanoma-associated chondroitin sulfate proteoglycan) was conducted in 2005.[186] Since the [^{213}Bi]Bi-cDTPA-9.2.27 was injected intralesional, high doses of up to 49.95 MBq (1350 μCi) were tolerable with no accumulation found in the kidneys. The author highlighted that intralesional TAT can be used for inoperable secondary melanoma or primary ocular melanoma.

In 2007, 22 patients with stage IV melanoma/in-transit metastasis were treated intravenously with the same radiolabelled bismuth immunoconjugate (55–947 MBq) to establish an effective dose.[187] A tolerable dose of 592 MBq with no renal damage was found. 20% of the patients showed partial or complete response (6% complete and 14% partially).

Building on the results gained from the phase I trial, another phase I study with 38 patients with end-stage metastatic melanoma was conducted by the same group in 2011.[188] The study extended the factors which may influence overall survival by investigating the melanoma-inhibitory activity protein, age, gender, disease stage and lactate dehydrogenase. The maximum injected does of 925 MBq did not cause any severe effects and thus, the maximum tolerance could not be determined. The phase I trial showed an overall 50% response rate and has the potential to be used as a treatment option for end-stage metastatic melanoma cancer.

The group of E. Dadachova injected intraperitoneally [^{213}Bi]Bi-CHX-A″-DTPA labelled (3.7 MBq μL^{-1}) mAb (8C3) targeting melanin alone and in combination with a standard drug for melanoma treatment (anti-CTLA4 mAb 9D9; 100 μg μL^{-1}), into tumour-bearing melanoma C57BL6 mice.[185] As an outcome, there was no synergistic effect observed when RIT was used in combination with immunotherapy. The authors justified it by the lack of anti-CTLA4 mAb efficacy in the murine model.

3.1.4 Myeloid leukemia. A systemic α immunotherapy study with 18 patients suffering from myeloid leukemia were treated with 10.36–37.0 MBq kg^{-1} [^{213}Bi]Bi-CHX-A″-DTPA-lintuzumab (anti-CD33).[206] Although an anti-leukemic effect could be measured in most of the patients, complete remission was not observed.

Eight years later the same group performed a phase I/II trial in 31 patients in combination with cytoreductive chemotherapy to test the maximum tolerated dose and antileukemia effect of [^{213}Bi]Bi-CHX-A″-DTPA-anti-CD33 (18.5–46.25 MBq kg^{-1}).[207] The authors claimed in both trials to administer alpha emitters with longer half-life to significantly enhance the therapeutic outcome.

3.1.5 Ovarian cancer. For the treatment of metastatic ovarian cancer, a radiolabelled HER2-targeting single domain antibody fragment (a2Rs15d) was investigated. The overall survival rate was studied in SKOV-3 xenografted mice by intravenously injection of fractionated administration of [^{213}Bi]Bi-DTPA-a2Rs15d (0.5–2 MBq) alone or in combination with trastuzumab.[208] Synergistic effects led to an increased median survival by applying three times 0.5 MBq in combination with trastuzumab compared to the control group. Biodistribution data was gained from Cherenkov radiation (from β decay and β decay of its daughters) and SPECT/CT imaging. High accumulation was not only found in the tumour (4.9 ± 0.05 %ID g^{-1} after 15 min p.i.), but also in the kidneys (59.9 ± 5.1 %ID g^{-1} after 60 min p.i.). By co-injection of gelofusine the uptake was reduced by 50%. However, the severe kidney uptake currently hinders translation into the clinic.

3.1.6 Neuroendocrine tumours (NETs) and pancreatic cancer. The conjugate [$^{205/206}$Bi][Bi(AAZTA-C4-TATE)]$^-$ was obtained quantitatively with a chelator concentration of 10^{-5} M at pH 3 at room temperature after 5 min of incubation. The conjugate was found to be stable in PBS, 10 mM DTPA and human plasma for 21 h. *In vivo* experiments in AR42 tumour bearing mice showed higher tumour uptake compared to [^{213}Bi][Bi(DOTA-TATE)]$^-$ (9.32 *vs.* 6.5 %ID g^{-1}) and reduced kidney uptake (10.1 *vs.* 17.4 %ID g^{-1}).[197] One initial clinical trial was performed using [^{213}Bi]Bi-DOTATOC in seven patients with NET pre-treated with ^{177}Lu and ^{90}Y and one with bone marrow carcinosis (Fig. 5). Successful treatment of all patients was achieved with even progression free survival up to 30 months after treatment.[199]

Novel proteins belonging to the family of Cancer/Testis Antigen (CTA) were developed to address the highly aggressive and to this stage incurable pancreatic ductal adenocarcinoma.[201] [^{213}Bi]Bi-CHX-A″-DTPA-labelled antibodies targeting CETN1 (centrin1) showed a tumour-specific uptake and effective treatment of intraperitoneally injected [^{213}Bi]Bi-CHX-A″-DTPA-labelled antibodies (single dose of 3.7 and 7.4 MBq) in MiaPaCa tumour-bearing mice. In comparison to the ^{177}Lu-labelled injected counterpart (same dose), only the alpha labelled mAb showed a reduced tumour growth rate pointing out that RIT is more effective than radionuclide therapy (RNT).

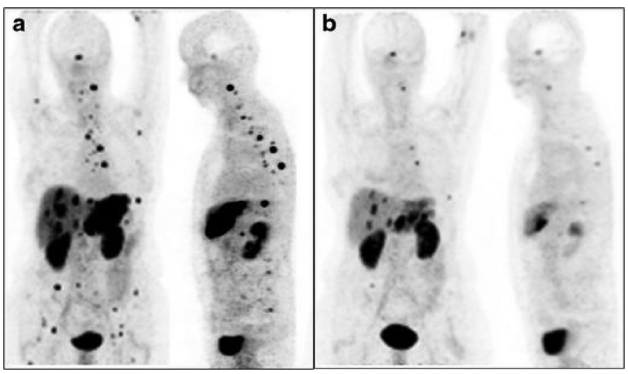

Fig. 5 (a) [^{68}Ga]Ga-DOTATOC-PET image of a patient with a tumour in the liver and metastases in the bone marrow as shown in coronal and sagittal maximum intensity projections. (B) Reduced tumour burden in the liver after treatment with 10.5 GBq [^{213}Bi]Bi-DOTATOC, as well as reduction of the bone metastases 6 month after treatment. (Reprinted with permission from ref. 199 Copyright 2014 Springer.)

3.1.7 Prostate cancer. Initial dose calculations for [^{213}Bi]Bi-DOTA-PSMA617 were performed based on [^{68}Ga]Ga-DOTA-TATE PET images from three patients. The dosimetry was found to be reasonable, but off-target accumulation, especially in the kidneys, was found to be even higher than for the respective ^{225}Ac or ^{177}Lu conjugates.[209]

However, a first patient with metastatic castration resistant prostate cancer (mCRPC) was treated with 592 MBq [^{213}Bi]Bi-DOTA-PSMA-617 given in two cycles. PSA levels were found to decrease from 237 μg L^{-1} to 43 μg L^{-1} eleven months post treatment (Table 3).[210]

3.2 Radiolabelled nanostructures

There are only limited reports on radiolabelled bismuth nanomaterials. The short half-life of $^{212/213}$Bi hinders the feasibility of implementation. An indirect strategy is the use of ^{212}Pb/^{212}Bi as an *in vivo* generator.[162]

The first study was reported by Diener *et al.*[211] They synthesised ^{212}Pb-labelled endohedral fullerenes by recoil synthesis following α decay and were further functionalized with malonic acid. The biodistribution behaviour was investigated in non-tumour bearing mice. A high uptake in the liver (53.7 ± 7.1 %ID g^{-1}) and spleen (27.2 ± 3.2 %ID g^{-1}) could be observed 8 h post injection and pointed to slow clearence from the body. The authors claimed that ^{212}Pb was encapsulated otherwise bone marrow uptake would have been observed.

Recently, ultrasmall silver telluride nanoparticles (~2 nm) were coated with gluthathion and radiolablled with ^{212}Pb without any chelator.[212] The [^{212}Pb]Pb-GSHAg$_2$Te showed high stability (~96% monitored by radio-TLC) in the presence of 1 mM EDTA after 24 h. However, these particles have not been investigated further neither *in vitro* nor *in vivo*.

One example of a ^{212}Bi-labelled nanostructure is reported by Kauffman *et al.*[213] They sucessfully labelled FDA-approved macroaggregated albumin (MAA) and investigated the conjugate *in vitro* and *in vivo* in breast cancer models based on 4T1 and EO771 cells. Reduction of tumour cell growth could be observed in both cell lines *in vitro* using clonogenic and survival assays. Biodistribution studies showed that after intratumoural administration, about 90% of the injected dose remains in 4T1 or EO771 orthotopic breast tumours in mice, resulting in a significant reduction in tumour size over a 18 day monitoring period.

4. Novel targeting/therapeutic strategies

Approaches to widen the spectrum of therapeutic conjugates by implementing a variety of molecules and nanomaterials

Table 3 Overview over preclinically and clinically investigated radiolabelled small molecules and antibodies

Preclinical					
Substance	Dose [MBq]	Tumour uptake [%ID g^{-1}]	Cytotoxic effects [%ID g^{-1}]	Disease	Ref.
[$^{205/206}$Bi]Bi-DOTA-IPB-NAPamide with and without 4-(*p*-iodo-phenyl)butyryl	2.39	4.50 ± 0.98/3.14 ± 0.32	8.78% ± 3.61 in kidneys	Melanoma	165
[^{213}Bi][Bi-Neunpa-Ph-Pip-Nle-CycMSH$_{hex}$)	0.1	5.91 ± 1.33	31.5 ± 4.99 in liver	Melanoma	171
[^{213}Bi]Bi-CHX-A″-DTPA-8C3	3.7 + 7.4	N/A	N/A	Melanoma	185
[$^{205/206}$Bi][Bi(AAZTA-C4-TATE)]	1.18	9.32 ± 3.96	10.1 in kidneys	NET	197
[^{213}Bi][Bi(DOTA-TATE)]	16.8 + 33.1	6.5 ± 2.3	17.4 ± 2.2 in kidneys	NET	197
[^{213}Bi]Bi-CHX-A″-DTPA-labelled antibodies targeting CETN1	3.7 + 7.4	N/A	N/A	NET	201
[^{213}Bi]Bi-DTPA-a2Rs15d	8.8 + 10.7	4.9 ± 0.05	59.9 ± 5.1 in kidneys	Ovarian cancer	208

Clinical				
Substance	Total administered dose [MBq]	Cytotoxic effects	Disease	Ref.
[^{213}Bi]Bi-CHX-A″-DTPA-anti-EGFR-mAb	366–821	—	Bladder cancer	169
[^{213}Bi]Bi-DOTA-SP	1400–9700	—	Glioma	183, 204 and 205
[^{213}Bi]Bi-DOTATOC	3300–20 600	Moderate hematological effects	NET	195
[^{213}Bi]Bi-cDTPA-9.2.27	592–925	—	Melanoma	186–188
[^{213}Bi]Bi-CHX-A″-DTPA-lintuzumab	1195–4755	10% treatment-related death 16% liver abnormalities	Myeloid leukemia	206 and 207
[^{213}Bi]Bi-DOTA-PSMA617	592	N/A	Prostate cancer	209 and 210

have been provided over the years and attempts to create synergistic effects in combination with other treatment options are still ongoing. A combination of radiation therapies with immunotherapeutic approaches, in particular, appears to be highly promising.[214] For example, beam irradiation or endogenous radiotherapies may result in the release of tumour associated antigens (TAA) from dying tumour cells.[215] Uptaken by dendritic cells, TAAs can be processed and presented by the immune system, thereby, leading to the activation of immune effector cells. This may explain the observed vaccination effects of radiotherapies against tumour cells, including in patients. For example, even non-irradiated tumour tissues become recognized by the immune system as a consequence of radiotherapy, also known as abscopal effect.[216] Besides vaccination, there is experimental evidence that irradiation of tumour tissues including by TAT[217] can enhance the entry of immune effector cells into tumour tissues, which can modulate the immunosuppressive tumour microenvironment (TME) to more inflammatory conditions, thereby facilitating the recognition of tumour cells by the immune system.[218–220] For these reasons it is expected that the combination of radiotherapy can improve immunotherapies including with bispecific antibodies (BsAb) or adoptive transfer of T cells genetically modified to express chimeric antigen receptors (CAR).[189,221]

Bearing in mind, (i) the above summarised potential applications of bismuth-based radiotheranostics on the one hand, and (ii) the promising data related to combined applications of radiotherapeutic strategies with immunotherapies on the other hand, novel bismuth-based immunotheranostics appear highly attractive and should therefore come into the focus of future pre-clinical and clinical evaluation. For these reasons, we include here an overview of such potential future combinatorial applications in the next chapter.

4.1 Immunotheranostics: history and future

Since the description of the magic bullets by Paul Ehrlich at the beginning of the 20th century,[222] for decades experimental immunotherapeutic approaches were developed for the treatment of tumours. Since the underlying mechanisms were not well understood such treatments were not reliable and difficult to reproduce. Therefore, tumour immunology was even considered as "alternative medicine". Even the development of monoclonal antibodies (mAbs), and later the detection of cellular immunity mediated by T-, NK and dendritic cells, did not lead to the anticipated major breakthrough of immunotherapies. The obvious drawback of murine mAbs is their weak interaction with both the human humoral and cellular immune effector mechanisms known as complement derived cytotoxicity (CDC), and antibody derived cellular cytotoxicity (ADCC). ADCC is mediated mainly by NK cells *via* the interaction of the Fc portion of the antibody with the Fc receptor expressed on immune cells. To overcome the limited cytotoxic capability of murine mAbs a variety of technologies were put forward, including for example the construction of immunodrug conjugates or radiolabelling of antibodies, as mentioned above. Limitations

still remain today: the most obvious problem of full-size antibodies is their pharmacology. Antibodies having an Ig format stay within the blood stream for several weeks. Due to the high osmotic pressure, their entry into the tumour tissues is difficult and takes around 4 to 48 h. In addition, ADCC is inhibited by the immunosuppressive environment inside of tumours. One of the next steps to overcome this limitation of full-size natural antibodies was the development of smaller antibody derived fragments such as the single fragment variables (scFvs) using upcoming recombinant antibody technologies. Alternatively, natural occurring small antibodies, so called nanobodies (nbs), from camelides or sharks came in the focus as potential immunotheranostics. However, their foreign immunogenic character leads to neutralization due to an immune response in humans. Besides, the pharmacokinetic of nbs and scFvs is also not favourable for usage as immune drug conjugate, either for imaging or therapy, as they are rapidly eliminated *via* the kidney, usually within 15 to 30 min after application. For this reason, only a low tumour enrichment can be achieved. So even now, and in spite of the dramatic progress made, there is still significant room for improvement in antibody based humoral or cellular immune therapies.

The first real major breakthrough of antibody-based immunotherapies was the detection of Abs that can release the brakes of the immune system,[223] which were termed as checkpoint inhibitors. The treatment of tumour patients with checkpoint inhibitors provided for the first-time convincing evidence for the tremendous potential of the humoral and cellular immune components to recognize and destroy tumour cells. In addition, it became obvious that tumour cells must have tricked the immune system and successfully circumvented all the obviously existing highly efficient natural immunological defence barriers when cancer is established in a patient.

Unfortunately, checkpoint inhibitors are only working against tumour cells that have collected manifold mutations during their evolution to become a tumour cell.[224] Therefore, scientists try nowadays to reinstall the capability of the immune system *via* the development of more efficient immunotherapeutic treatment modalities based on vaccination, immunotheranostic compounds including BsAb, modified advanced nanomaterials, and most recently another major breakthrough using immune cells genetically modified to express chimeric artificial receptors (CARs).[225]

4.1.1 Overview on immunotherapeutic approaches

Bispecific antibodies. Bispecific antibodies (BsAbs) for tumour therapies are usually directed to a tumour associated antigen (TAA, *e.g.* CD19), which is overexpressed on the surface of a tumour cell, and also to an activating receptor (*e.g.* CD3) on the cell surface of an immune effector cell. BsAbs can be constructed from the variable domains of the heavy and light chains of two monoclonal antibodies (mAbs). The domains of both mAbs are recombinantly fused to form single chain fragment variables (scFv), which are then fused to form the BsAb. BsAb can cross-link T cells with target cells, which finally leads to the destruction of the tumour cell. A schematic overview is shown in Fig. 6 (upper panel).

Conventional CARs. Conventional CARs consist of three domains: (i) an extracellular antibody-based domain, usually in the scFv format (ii) a transmembrane domain, and (iii) intracellular signalling domains. Via the extracellular antibody domain CAR T cells can bind to the TAA on the surface of the tumour cell and destroy it (Fig. 6 lower panel).

For CAR T immunotherapy, T cells are isolated from the patient and transduced with the gene encoding the respective CAR construct. The resulting genetically modified CAR T cells are then adoptively transferred back into the patient.

The idea to equip T cells with an antibody based artificial receptor was already described at the end of the 1980s.[226] However, it took decades of development until their more recent successful clinical application and first approvals by the respective legal authorities.

Although the CAR T cell technology remains extremely expensive, an impressive number of patients have been successfully treated with such individualised living drugs. While the positive outcome of CAR T cell treatments have underlined their high potential, their limitations have also become evident: activated CAR T cells strongly proliferate and produce high amounts of cytokines. As a consequence, CAR T cell treatments are associated with a high risk of severe life-threatening side effects, including cytokine release syndrome (CRS). In addition, OFF tumour On target effects can occur as the expression of the targeted TAA is usually not limited to the tumour cell but may also occur on the surface of healthy tissues.

Despite their side effects, the specificity of conventional CAR T cells is limited to just one target, which facilitates the development of tumour cell escape mechanisms.

Adaptor CARs. To overcome these problems, we and others have developed modular CAR T cell treatment platforms, nowadays known as adaptor CAR T cells. Starting from a modular BsAb approach, which we termed the UniMAB system (Fig. 7, left panel),[227] we have established two versions of adaptor CAR platforms which we term the UniCAR and RevCAR system (patents[228–230]) (Fig. 7, right panel).[221,225] For both adaptor CAR platforms proof of functionality has not only been shown in pre-clinical *in vitro* and *in vivo* studies[231,232] but also in currently running clinical phase 1 trials (UniCAR: NCT04230265; NCT04633148; RevCAR: NCT05949125).

In contrast to conventional CAR T cells, which are permanently active after adoptive transfer of the genetically modified immune cells, the function of adaptor CAR T cells depends on the presence of a bridging molecule (target module, TM), which is required for the cross-linkage of the adaptor CAR T cell with the tumour cell (Fig. 7). This strategy allows a repeated stop and go treatment *via* regulation of the infusion of the respective TM (Fig. 8).

Obviously, the pharmacokinetics of the respective TM determines the efficiency and safety profile of adapter CAR T cells. TMs that can be rapidly eliminated allow a fast turning OFF of the adaptor CAR T cells. However, the downside is that their

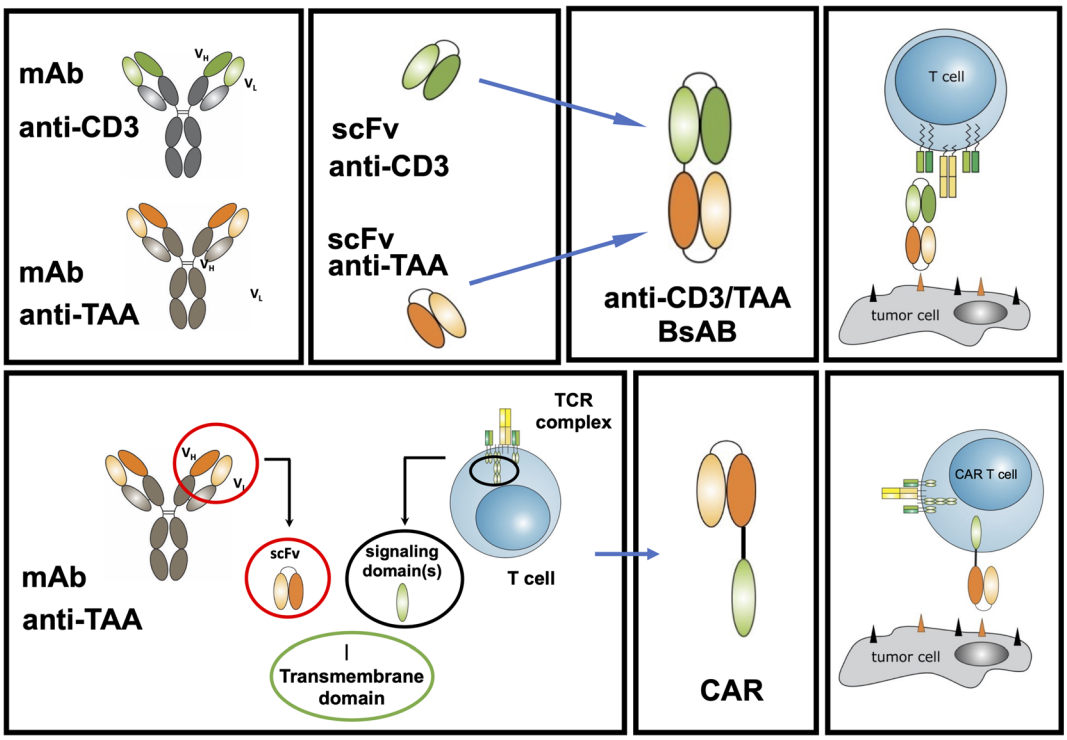

Fig. 6 Construction and retargeting of immune cells with BsAbs (upper panel) and conventional CAR T cells (lower panel). ScFvs can be constructed from the variable domains of two mAbs and fused to a BsAb. Cross-linkage *via* the BsAb leads to the killing of the tumour cell by the redirected T cell. A conventional CAR consists of three portions, the extracellular domain targeting a TAA usually a scFv directed to a TAA, a transmembrane domain and intracellular signalling domains taken from activatory receptors of the T cell receptor complex. The gene encoding such an artificial receptor can be transduced into T cells. The resulting CAR T cells can recognize tumour cells *via* their extracellular antibody domain. The interaction with the target cell leads to the formation of an artificial immune synapse, which finally triggers the cell death of the tumour cell.

application requires a permanent infusion to achieve the TM concentration necessary for efficiency. During treatment, the patient is hospitilized at an intensive care unit, which is obviously not convenient for the patient. *Vice versa*, a TM having an extended half-life would facilitate the application for the patient but increases the risk of severe site-effects as adaptor CARs targeting TMs based on full size antibodies will behave more or less like non-regulatable conventional CARs.

For the UniCAR and RevCAR platforms, we have therefore developed a series of TMs having different pharmacokinetic profiles, which is achieved by the construction of molecules having different molecular weight.[221] A revised treatment modality with UniCAR or RevCAR T cells would start with TMs having a short half live allowing a fast interruption of the T cell function if necessary. Once most of the tumour load has been destroyed and the risk of CRS becomes low, a TM having a long half live could be applied. Although feasible and working in *in vitro* and *in vivo* models, the need for different TMs would obviously enhance the cost for the development of the respective GMP grade TMs and would require additional clinical trials.

Conjugation of TMs with Bi-NMs may not only be useful for optimization of the pharmacokinetic properties of TMs but also for imaging of tumours and therapeutic treatments. Furthermore, radioactive versions could help to overcome the immunosuppressive tumour microenvironment.

5. Outlook and conclusion

Recent advances in cancer therapies, integrating metals to precisely target cancer cells for effective imaging and therapy, are transforming the modern therapeutics. Towards this goal, bismuth in its various forms, has garnered much attention as a non-toxic and highly stable metal with many fascinating properties. The clinical application of small bismuth complexes appears to be feasible as only minor side effects, if at all, were observed when these compounds were carefully applied.[2,8] Kidney damage was only seen in the event of an overdose.[233] Overall, the lower toxicity but also higher cost-effectiveness of bismuth-based materials compared to common precious metal-based anticancer compounds has led to an emerging rush towards commercialization. In the field of bismuth-containing nanomaterials, there are also promising developments that would justify clinical use. For example, the CT contrast of Bi-NMs is significantly higher than that of clinically approved iodine-based contrast agents, the photoconversion efficiency is very high and there are targeted materials available that achieve high tumour accumulation. However, to our knowledge, no clinical studies with Bi-NMs have been conducted to date. In the future, extensive clinical studies will be required here, with scientists, physicians and stakeholders of regulatory authority having to work closely together. In particular, the

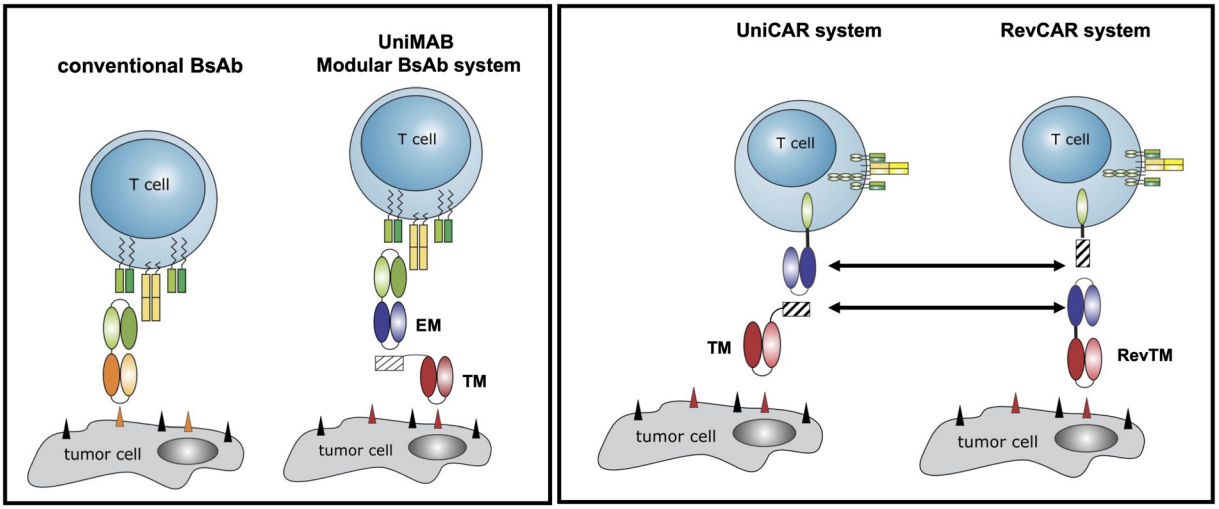

Fig. 7 Originally, to accelerate the development of conventional BsAbs, we established the modular bispecific antibody platform UniMAB. For this purpose, we decided to split the BsAB into two components, an effector module (EM) and a targeting module (TM). The EM is a bispecific antibody, which recognizes on the one hand an activating domain of the immune cell (*e.g.* CD3) and on the other hand a peptide epitope. This epitope sequence is part of the TM. Thus, EM and TM can form an immune complex with properties similar to conventional BsAbs. This is the same strategy as we later used for our adaptor CAR platform technologies UniCAR and RevCAR. In contrast to conventional CARs, UniCARs do not recognize a TAA directly on the surface of a tumour cell but the same peptide epitope as the EM of the UniMAB system. Consequently, UniCAR T cells can establish an interaction with tumour cells *via* the same TMs used in the UniMAB system.[221] The RevCAR system differs from the UniCAR system as follows: the scFv domain of the UniCAR is replaced by the peptide epitope and *vice versa* the epitope tag in the TM is replaced by the anti-peptide epitope scFv.

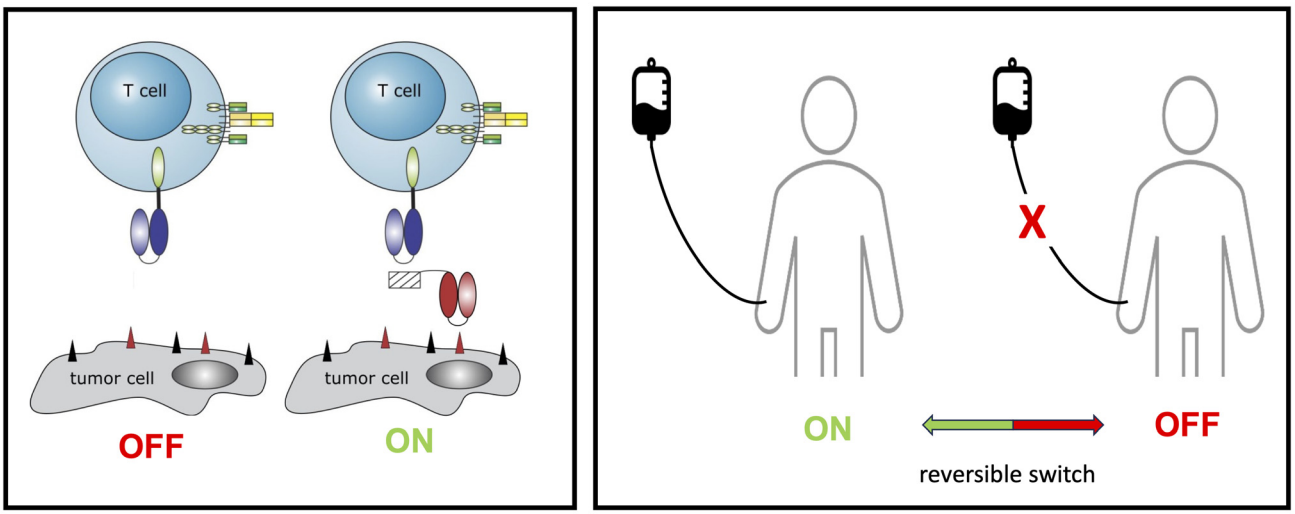

Fig. 8 UniCAR (and RevCAR T cells) are inactive in the absence of a TM. They can be turned on by adding of the TM and turned OFF by elimination of the TM. In the clinical setting TMs are applied by continuous infusion. In case of side effects, the infusion can be stopped and thereby the function of the UniCAR T cells (RevCAR T cells) can be turned OFF. The adaptor CAR T cells can be restarted by further infusion of the TM. An additional advantage of adaptor CARs is the chance to apply an alternative TM with a different specificity in case tumour escape variants occur.

fabrication of nanomaterials under the conditions of good manufacturing practice (GMP) is a challenge. However, in the meantime, the art of synthesis in this field has progressed considerably.

At the nanoscale, bismuth is known for its effective radiosensitising and strong photothermal conversion properties as well as its remarkable performance as a strong contrast agent for various imaging modalities including CT, IRT, PA and MRI. In the field of imaging, ultrasmall particles (<6 nm) with appropriate surface functionalisation are becoming increasingly important because, they can reach all parts of the body and are quickly excreted by the kidneys.[234] Additionally, Bi-NPs can be functionalised with various targeting agents and coating molecules to generate well-defined and site-targeted Bi-NPs for therapeutic applications on the basis of PTT, PDT and RT. Besides imaging, another highly attractive feature of

Bi-based materials is based on the existence of radioactive bismuth compounds. Such radiobismuth compounds conjugated for instance with small molecules like peptides are highly promising radiopharmaceuticals including for endoradionuclide therapy.

With clinical applications in patients in mind, it is noteworthy to mention that the surface of Bi-NPs can be designed to prevent the formation of a protein corona and thus avoid off-target effects.[235] Besides well-known biological vector molecules such as specific peptides and antibodies and their fragments, there is the possibility of using cancer cell membranes for targeting. A major problem with the introduction of new materials into the clinic still remains the dilemma of nanotoxicity.[236] But with no doubt, nanomaterials and especially Bi-NPs may lead to promising novel treatment modalities for the imaging and treatment of otherwise fatal diseases for which global unmet medical needs exists. The currently remaining problems may hopefully be solved in the near future through interdisciplinary collaboration and partnerships across various disciplines.[237]

One example of a success story of interdisciplinary cooperation is currently the development of tumours therapies based on combinations of cytostatic drugs, radio-, and immunotherapies. Bearing in mind that local beam or endoradionuclide-based irradiation or the treatment with cytostatic drugs does not only lead to cell death but also alters the tumour microenvironment from immunosuppressive to inflammation, combinations of modern immunotherapeutic approaches based on BsAbs or CAR T cell technologies with well-established conventional tumour therapies appear very promising. Also, combinations with immunotheranostics and/or radiosensitisers based on advanced nanomaterials represent highly promising strategies to further improve the efficacy of future tumour immunotherapies. Due to the above summarized interesting features, bismuth-based nanoparticles may become of special interest and should therefore be tested in the near future in combination with BsAbs, modular BsAbs, CAR T cells, and the adaptor CAR T cell platforms UniCAR and RevCARs. TMs for adaptor CAR T cells could be constructed, consisting of Bi-NPs conjugated with both the antibody domain against a TAA and the peptide epitope recognized by an adaptor CAR T cell (Fig. 9).

In summary, this perspective provides an overview of different types of Bi-NMs, such as metallic Bi-NPs, Bi-chalcogenides and Bi-hybrid structures that are relevant for clinical applications, and discusses key examples of colloidal stable, biocompatible and efficacious anti-cancer Bi-NPs and its related forms. Moreover, an overview of developments in radiobismuth-labelled compounds for targeted alpha therapy are presented, highlighting specific examples of radiolabelled bioconjugates and nanomaterials engineered for selective tumour treatment. A potential construction of Bi-NPs based TMs for multimodal usage in combination with adaptor CAR T cell technologies for cellular immunotherapy approaches of tumours are also presented. Using such Bi-NP based TMs may not only allow an optimisation of the pharmacokinetic properties of TMs but the modulation of the tumour microenvironment towards an improved attraction, invasion and killing efficacy of adaptor CAR T cells and thereby be helpful to overcome current limitations of cellular immunotherapies. These insights into the anti-cancer potential of Bi-materials offer a strong foundation for future research in cancer diagnostics and therapy, with the potential to drive the clinical implementation of Bi-based materials for cancer (immuno)theranostics.

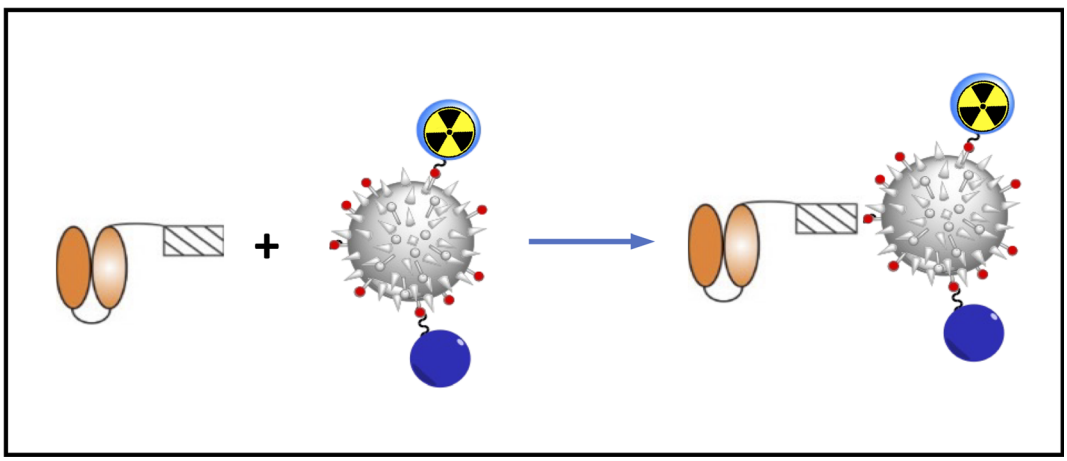

Fig. 9 Multimodal (Bi based) NP can be constructed and conjugated with TMs to optimize their pharmacokinetic properties. Radioactively labelled TM versions could be used to modulate the tumour microenvironment from immunosuppressive to inflammation. Besides such Bi based NP could also be used for imaging of tumours and of the therapeutic effects: Bi-NPs based TMs could be established and equipped with additional features, for example *via* conjugation of small molecules or recombinant antibody derivatives to Bi-NPs, the pharmacokinetic property of a TM could be altered and fine-tuned. Radioactive versions of Bi-NP based TMs could directly modulate the tumour microenvironment from immunosuppressive towards inflammation as a prerequisite for attraction, invasion and activation of adaptor CAR T cells.

Data availability

This is a perspective article that contains no original data.

Conflicts of interest

There are no conflicts to declare.

Acknowledgements

We are grateful for the excellent work carried out by co-workers and colleagues mentioned in the references, specifically the groups in the MHELTHERA consortium. For financial support, we acknowledge Helmholtz-Zentrum Dresden-Rossendorf, the Australian Research Council (DP220103632), Monash University, and in particular the Helmholtz Initiative and Networking Fund (Radio-Immuno-Theranostics (MHELTHERA) project ID: InterLabs-0031).

References

1 R. Mohan, *Nat. Chem.*, 2010, **2**, 336–336.
2 Â. Gonçalves, M. Matias, J. A. R. Salvador and S. Silvestre, *Int. J. Mol. Sci.*, 2024, **25**, 1600.
3 J. A. Salvador, S. A. Figueiredo, R. M. Pinto and S. M. Silvestre, *Future Med. Chem.*, 2012, **4**, 1495–1523.
4 G. G. Briand and N. Burford, *Chem. Rev.*, 1999, **99**, 2601–2658.
5 K. D. Mjos and C. Orvig, *Chem. Rev.*, 2014, **114**, 4540–4563.
6 D. M. Griffith, H. Li, M. V. Werrett, P. C. Andrews and H. Sun, *Chem. Soc. Rev.*, 2021, **50**, 12037–12069.
7 R. Ge and H. Sun, *Acc. Chem. Res.*, 2007, **40**, 267–274.
8 J. D. S. Rosário, F. H. Moreira, L. H. F. Rosa, W. Guerra and P. P. Silva-Caldeira, *Molecules*, 2023, **28**, 5921.
9 K. Iuchi, S. Shirai, Y. Tasaki and H. Hisatomi, *Anti-Cancer Drugs*, 2020, **31**, 55–59.
10 Y.-P. Liu, J. Lei, L.-W. Tang, Y. Peng, C.-T. Au, Y. Chen and S.-F. Yin, *Eur. J. Med. Chem.*, 2017, **139**, 826–835.
11 K. Iuchi and T. Yagura, *Toxicol. in Vitro*, 2018, **50**, 172–178.
12 K. Iuchi, Y. Tasaki, S. Shirai and H. Hisatomi, *Biomed. Pharmacother.*, 2020, **125**, 109928.
13 K. Iuchi, Y. Hatano and T. Yagura, *Biochem. Pharmacol.*, 2008, **76**, 974–986.
14 Y.-K. Li, M. Yang, M.-X. Li, H. Yu, H.-C. Wu and S.-Q. Xie, *Bioorg. Med. Chem. Lett.*, 2013, **23**, 2288–2292.
15 M. Arda, I. I. Ozturk, C. N. Banti, N. Kourkoumelis, M. Manoli, A. J. Tasiopoulos and S. K. Hadjikakou, *RSC Adv.*, 2016, **6**, 29026–29044.
16 P. F. Chan, K. P. Ang and R. A. Hamid, *BioMetals*, 2021, **34**, 365–391.
17 K. Onishi, M. Douke, T. Nakamura, Y. Ochiai, N. Kakusawa, S. Yasuike, J. Kurita, C. Yamamoto, M. Kawahata, K. Yamaguchi and T. Yagura, *J. Inorg. Biochem.*, 2012, **117**, 77–84.
18 P. F. Chan, K. P. Ang and R. A. Hamid, *JBIC, J. Biol. Inorg. Chem.*, 2024, **29**, 217–241.
19 D. H. A. Ishak, K. K. Ooi, K.-P. Ang, A. M. Akim, Y.-K. Cheah, N. Nordin, S. N. B. A. Halim, H.-L. Seng and E. R. T. Tiekink, *J. Inorg. Biochem.*, 2014, **130**, 38–51.
20 A. Islam, B. L. Rodrigues, I. M. Marzano, E. C. Perreira-Maia, D. Dittz, M. T. Paz Lopes, M. Ishfaq, F. Frézard and C. Demicheli, *Eur. J. Med. Chem.*, 2016, **109**, 254–267.
21 M. López-Cardoso, H. Tlahuext, M. Pérez-Salgado, D. G. Vargas-Pineda, P. P. Román-Bravo, A. M. Cotero-Villegas, M. Acevedo-Quiroz, R. S. Razo-Hernández, P. Alvarez-Fitz, M. A. Mendoza-Catalán, V. Jancik and R. Cea-Olivares, *J. Mol. Struct.*, 2020, **1217**, 128456.
22 I. M. Marzano, D. Tomco, R. J. Staples, E. H. Lizarazo-Jaimes, D. A. Gomes, M. Bucciarelli-Rodriguez, W. Guerra, Í. P. De Souza, C. N. Verani and E. C. Pereira Maia, *J. Inorg. Biochem.*, 2021, **222**, 111522.
23 S. Yarar, I. I. Ozturk, C. N. Banti, N. Panagiotou, C. Papatriantafyllopoulou, M. Manoli, M. J. Manos, A. J. Tasiopoulos and S. K. Hadjikakou, *Inorg. Chim. Acta*, 2018, **471**, 23–33.
24 N. Zhang, Y. Tai, M. Li, P. Ma, J. Zhao and J. Niu, *Dalton Trans.*, 2014, **43**, 5182.
25 E. R. T. Tiekink, *Crit. Rev. Oncol. Hematol.*, 2002, **42**, 217–224.
26 H. Li, C. S. Lai, J. Wu, P. C. Ho, D. De Vos and E. R. T. Tiekink, *J. Inorg. Biochem.*, 2007, **101**, 809–816.
27 A. Kumar Singh, A. Kumar, H. Singh, P. Sonawane, P. Pathak, M. Grishina, J. Pal Yadav, A. Verma and P. Kumar, *Chem. Biodiversity*, 2023, **20**, e202300061.
28 R. Ouyang, Y. Yang, X. Tong, K. Feng, Y. Yang, H. Tao, X. Zhang, T. Zong, P. Cao, F. Xiong, N. Guo, Y. Li, Y. Miao and S. Zhou, *J. Inorg. Biochem.*, 2017, **168**, 18–26.
29 X. Jia, J. Pang, Y. Chu, S. Li, W. Li, M. Jiang and F. Yang, *J. Mol. Struct.*, 2024, **1318**, 139389.
30 P. C. Andrews, G. B. Deacon, C. M. Forsyth, P. C. Junk, I. Kumar and M. Maguire, *Angew. Chem., Int. Ed.*, 2006, **45**, 5638–5642.
31 D. C. Senevirathna, M. V. Werrett, M. Kubeil, H. Stephan and P. C. Andrews, *Dalton Trans.*, 2019, **48**, 15962–15969.
32 Y. Cheng and H. Zhang, *Chem. – Eur. J.*, 2018, **24**, 17405–17418.
33 S. Badrigilan, J. Choupani, H. Khanbabaei, M. Hoseini-Ghahfarokhi, T. J. Webster and L. Tayebi, *Adv. Healthcare Mater.*, 2020, **9**, 1901695.
34 Q. Wang, J. Du, R. Ouyang, B. Liu, Y. Miao and Y. Li, *Coord. Chem. Rev.*, 2023, **492**, 215281.
35 O. Rabin, J. Manuel Perez, J. Grimm, G. Wojtkiewicz and R. Weissleder, *Nat. Mater.*, 2006, **5**, 118–122.
36 Y. Liu, P. Bhattarai, Z. Dai and X. Chen, *Chem. Soc. Rev.*, 2019, **48**, 2053–2108.
37 B. B. Lahiri, S. Bagavathiappan, T. Jayakumar and J. Philip, *Infrared Phys. Technol.*, 2012, **55**, 221–235.

38 D. Kesztyüs, S. Brucher, C. Wilson and T. Kesztyüs, *Medicina*, 2023, **59**, 2139.
39 W. Li, Y. Fan, J. Lin, P. Yu, Z. Wang and C. Ning, *Adv. Ther.*, 2022, **5**, 2200027.
40 M. Kowalik, J. Masternak and B. Barszcz, *Curr. Med. Chem.*, 2019, **26**, 729–759.
41 N. Kavousi, M. Nazari, M. T. B. Toossi, H. Azimian and M. Alibolandi, *J. Drug Delivery Sci. Technol.*, 2024, **101**, 106136.
42 J. Xie, L. Gong, S. Zhu, Y. Yong, Z. Gu and Y. Zhao, *Adv. Mater.*, 2019, **31**, 1802244.
43 T. I. Kostelnik and C. Orvig, *Chem. Rev.*, 2019, **119**, 902–956.
44 G. Sgouros, L. Bodei, M. R. McDevitt and J. R. Nedrow, *Nat. Rev. Drug Discovery*, 2020, **19**, 589–608.
45 D. Shahbazi-Gahrouei, Y. Choghazardi, A. Kazemzadeh, P. Naseri and S. Shahbazi-Gahrouei, *IET Nanobiotechnol.*, 2023, **17**, 302–311.
46 J.-J. Xu, W.-C. Zhang, Y.-W. Guo, X.-Y. Chen and Y.-N. Zhang, *Drug Delivery*, 2022, **29**, 664–678.
47 A. Hheidari, J. Mohammadi, M. Ghodousi, M. Mahmoodi, S. Ebrahimi, E. Pishbin and A. Rahdar, *Front. Bioeng. Biotechnol.*, 2024, **12**, 1436297.
48 R. Khursheed, K. Dua, S. Vishwas, M. Gulati, N. K. Jha, G. M. Aldhafeeri, F. G. Alanazi, B. H. Goh, G. Gupta, K. R. Paudel, P. M. Hansbro, D. K. Chellappan and S. K. Singh, *Biomed. Pharmacother.*, 2022, **150**, 112951.
49 G. Jia, Y. Wang, M. Sun, H. Zhang, L. Li, Y. Shi, L. Zhang, X. Cui, T. W. B. Lo, B. Huang and J. C. Yu, *J. Am. Chem. Soc.*, 2023, **145**, 14133–14142.
50 D. Leng, T. Wang, Y. Li, Z. Huang, H. Wang, Y. Wan, X. Pei and J. Wang, *Inorg. Chem.*, 2021, **60**, 17258–17267.
51 I. Khan, K. Saeed and I. Khan, *Arabian J. Chem.*, 2019, **12**, 908–931.
52 Á. Y. Aguilera, G. Krepper and M. S. Di Nezio, *J. Cluster Sci.*, 2022, **33**, 1417–1426.
53 J. Wu, F. Qin, Z. Lu, H.-J. Yang and R. Chen, *Nanoscale Res. Lett.*, 2011, **6**, 66.
54 M. Mahiuddin and B. Ochiai, *RSC Adv.*, 2021, **11**, 26683–26686.
55 C. Liu, L. Zhang, X. Chen, S. Li, Q. Han, L. Li and C. Wang, *Chem. Eng. J.*, 2020, **382**, 122720.
56 L. Jiao, Q. Li, J. Deng, N. Okosi, J. Xia and M. Su, *Nanoscale*, 2018, **10**, 6751–6757.
57 Y. Xuan, X. Q. Yang, Z. Y. Song, R. Y. Zhang, D. H. Zhao, X. L. Hou, X. L. Song, B. Liu, Y. D. Zhao and W. Chen, *Adv. Funct. Mater.*, 2019, **29**, 1900017.
58 M. Shakibaie, H. Forootanfar, A. Ameri, M. Adeli-Sardou, M. Jafari and H. R. Rahimi, *IET Nanobiotechnol.*, 2018, **12**, 653–657.
59 Z. Saddique, M. Imran, A. Javaid, S. Latif, T. H. Kim, M. Janczarek, M. Bilal and T. Jesionowski, *Environ. Res.*, 2023, **229**, 115861.
60 C. Gomez, G. Hallot, A. Pastor, S. Laurent, E. Brun, C. Sicard-Roselli and M. Port, *Ultrason. Sonochem.*, 2019, **56**, 167–173.
61 R. Ouyang, Q. Zhang, P. Cao, Y. Yang, Y. Zhao, B. Liu, Y. Miao and S. Zhou, *Colloids Surf., B*, 2023, **222**, 113116.
62 M. Baričić, J. M. Nuñez, M. H. Aguirre, D. Hrabovsky, M. Seydou, C. Meneghini, D. Peddis and S. Ammar, *Sci. Rep.*, 2024, **14**, 12529.
63 S. Ammar and F. Fiévet, *Nanomaterials*, 2020, **10**, 1217.
64 S. Yang, Z. Li, Y. Wang, X. Fan, Z. Miao, Y. Hu, Z. Li, Y. Sun, F. Besenbacher and M. Yu, *ACS Appl. Mater. Interfaces*, 2018, **10**, 1605–1615.
65 Q. Bao, Y. Zhang, X. Liu, T. Yang, H. Yue, M. Yang and C. Mao, *Adv. Opt. Mater.*, 2023, **11**, 2201482.
66 D. Sun, S. Zhou and W. Gao, *ACS Nano*, 2020, **14**, 12281–12290.
67 H. Xiang, Y. Wu, X. Zhu, M. She, Q. An, R. Zhou, P. Xu, F. Zhao, L. Yan and Y. Zhao, *J. Am. Chem. Soc.*, 2021, **143**, 11449–11461.
68 J. Fang, H. Nakamura and H. Maeda, *Adv. Drug Delivery Rev.*, 2011, **63**, 136–151.
69 S. K. Golombek, J.-N. May, B. Theek, L. Appold, N. Drude, F. Kiessling and T. Lammers, *Adv. Drug Delivery Rev.*, 2018, **130**, 17–38.
70 A. Nel, E. Ruoslahti and H. Meng, *ACS Nano*, 2017, **11**, 9567–9569.
71 Y. Huang, Z. Xue and S. Zeng, *ACS Appl. Mater. Interfaces*, 2020, **12**, 31172–31181.
72 X. Yu, A. Li, C. Zhao, K. Yang, X. Chen and W. Li, *ACS Nano*, 2017, **11**, 3990–4001.
73 J. Deng, S. Xu, W. Hu, X. Xun, L. Zheng and M. Su, *Biomaterials*, 2018, **154**, 24–33.
74 X. Ren, S. Yang, N. Yu, A. Sharjeel, Q. Jiang, D. K. Macharia, H. Yan, C. Lu, P. Geng and Z. Chen, *J. Colloid Interface Sci.*, 2021, **591**, 229–238.
75 P. Lei, R. An, P. Zhang, S. Yao, S. Song, L. Dong, X. Xu, K. Du, J. Feng and H. Zhang, *Adv. Funct. Mater.*, 2017, **27**, 1702018.
76 R. Vazquez-Munoz, M. J. Arellano-Jimenez and J. L. Lopez-Ribot, *BMC Biomed. Eng.*, 2020, **2**, 11.
77 J. C. Bulmahn, G. Tikhonowski, A. A. Popov, A. Kuzmin, S. M. Klimentov, A. V. Kabashin and P. N. Prasad, *Nanomaterials*, 2020, **10**, 1463.
78 M. B. Larosi, J. D. V. García and A. R. Rodríguez, *Nanomaterials*, 2022, **12**, 2903.
79 H. Bi, F. He, Y. Dong, D. Yang, Y. Dai, L. Xu, R. Lv, S. Gai, P. Yang and J. Lin, *Chem. Mater.*, 2018, **30**, 3301–3307.
80 K. Zarschler, L. Rocks, N. Licciardello, L. Boselli, E. Polo, K. P. Garcia, L. De Cola, H. Stephan and K. A. Dawson, *Nanomedicine*, 2016, **12**, 1663–1701.
81 C. Yang, C. Guo, W. Guo, X. Zhao, S. Liu and X. Han, *ACS Appl. Nano Mater.*, 2018, **1**, 820–830.
82 C. Liu, Y. Zhang, J. Wen, J. Liu, M. Huo, Y. Shen, H. Luo and H. Zhang, *J. Drug Targeting*, 2024, 1–13, DOI: **10.1080/1061186x.2024.2329110**.
83 R. Singh, P. Kumari, M. Kumar, T. Ichikawa and A. Jain, *Molecules*, 2020, **25**, 3733.
84 J. Deng and Z.-Y. Zhao, *Comput. Mater. Sci.*, 2018, **142**, 312–319.

85 W. W. Anku, S. O. B. Oppong and P. P. Govender, *Bismuth-Based Nanoparticles as Photocatalytic Materials*, *InTech*, 2018, DOI: 10.5772/intechopen.75104.
86 M. Batool, M. F. Nazar, A. Awan, M. B. Tahir, A. Rahdar, A. E. Shalan, S. Lanceros-Méndez and M. N. Zafar, *Nano-Struct. Nano-Objects.*, 2021, **27**, 100762.
87 J. Ni, X. Bi, Y. Jiang, L. Li and J. Lu, *Nano Energy*, 2017, **34**, 356–366.
88 T. O. Ajiboye, O. A. Oyewo and D. C. Onwudiwe, *Surf. Interfaces*, 2021, **23**, 100927.
89 J. Huang, Q. Huang, M. Liu, Q. Chen and K. Ai, *Front. Pharmacol.*, 2022, **13**, 844037.
90 J. Jiang, X. Che, Y. Qian, L. Wang, Y. Zhang and Z. Wang, *Front. Mater.*, 2020, **7**, 234.
91 M. Dastgir, Y. Ayyami, A. Pourfarshid, M. Ghorbani and T. Mortezazadeh, *J. Drug Delivery Sci. Technol.*, 2024, **92**, 105279.
92 M.-A. Shahbazi, L. Faghfouri, M. P. A. Ferreira, P. Figueiredo, H. Maleki, F. Sefat, J. Hirvonen and H. A. Santos, *Chem. Soc. Rev.*, 2020, **49**, 1253–1321.
93 Y. He, H. Chen, W. Li, L. Xu, H. Yao, Y. Cao, Z. Wang, L. Zhang, D. Wang and D. Zhou, *J. Nanobiotechnol.*, 2023, **21**, 209.
94 K. Poudel, A. Banstola, M. Gautam, Z. C. Soe, L. M. Pham, J.-H. Jeong, H.-G. Choi, S. K. Ku, C. S. Yong, T. H. Tran and J. O. Kim, *Nanoscale*, 2021, **13**, 1231–1247.
95 L. Li, Y. Lu, C. Jiang, Y. Zhu, X. Yang, X. Hu, Z. Lin, Y. Zhang, M. Peng, H. Xia and C. Mao, *Adv. Funct. Mater.*, 2018, **28**, 1704623.
96 N. N. Talik Sisin, K. Abdul Razak, S. Zainal Abidin, N. F. Che Mat, R. Abdullah, R. Ab Rashid, M. A. Khairil Anuar and W. N. Rahman, *Int. J. Nanomed.*, 2020, 7805–7823.
97 Z. Song, T. Liu, H. Lai, X. Meng, L. Yang, J. Su and T. Chen, *ACS Nano*, 2022, **16**, 4379–4396.
98 C. Yang, Y. Chen, W. Guo, Y. Gao, C. Song, Q. Zhang, N. Zheng, X. Han and C. Guo, *Adv. Funct. Mater.*, 2018, **28**, 1706827.
99 J. Du, Z. Gu, L. Yan, Y. Yong, X. Yi, X. Zhang, J. Liu, R. Wu, C. Ge, C. Chen and Y. Zhao, *Adv. Mater.*, 2017, **29**, 1701268.
100 J. Liu, X. Zheng, L. Yan, L. Zhou, G. Tian, W. Yin, L. Wang, Y. Liu, Z. Hu and Z. Gu, *ACS Nano*, 2015, **9**, 696–707.
101 X. Zheng, J. Shi, Y. Bu, G. Tian, X. Zhang, W. Yin, B. Gao, Z. Yang, Z. Hu, X. Liu, L. Yan, Z. Gu and Y. Zhao, *Nanoscale*, 2015, **7**, 12581–12591.
102 Y. Chen, G. Zhao, S. Wang, Y. He, S. Han, C. Du, S. Li, Z. Fan, C. Wang and J. Wang, *Biomater. Sci.*, 2019, **7**, 3450–3459.
103 X. Cheng, Y. Yong, Y. Dai, X. Song, G. Yang, Y. Pan and C. Ge, *Theranostics*, 2017, **7**, 4087–4098.
104 Y. Cheng, Y. Chang, Y. Feng, H. Jian, X. Wu, R. Zheng, K. Xu and H. Zhang, *Adv. Mater.*, 2019, **31**, 1806808.
105 H. Zhang, G. Chen, B. Yu, Y. Shen and H. Cong, *ACS Appl. Bio Mater.*, 2019, **2**, 3870–3876.
106 F. Akbarzadeh, K. Khoshgard, E. Arkan, L. Hosseinzadeh and A. Hemati Azandaryani, *Artif. Cells, Nanomed., Biotechnol.*, 2018, **46**, S514–S523.
107 F. Akbarzadeh and K. Khoshgard, *Photodiagn. Photodyn. Ther.*, 2024, **46**, 104025.
108 J. Bai, X. Jia, Y. Ruan, C. Wang and X. Jiang, *Inorg. Chem.*, 2018, **57**, 10180–10188.
109 Y. Ma, D.-Y. Zhang, Z. Peng, S. Guan and J. Zhai, *Mol. Pharm.*, 2020, **17**, 3403–3411.
110 F. Du, J. Lou, R. Jiang, Z. Fang, X. Zhao, Y. Niu, S. Zou, M. Zhang, A. Gong and C. Wu, *Int. J. Nanomed.*, 2017, **12**, 5973–5992.
111 Y. Lu, L. Li, Z. Lin, M. Li, X. Hu, Y. Zhang, M. Peng, H. Xia and G. Han, *Adv. Healthcare Mater.*, 2018, **7**, 1800602.
112 G. Chen, Z. Yang, J. Du, Z. He, Y. Zhang, K. Zheng, S. Cai, M. Chen, Y. Li, L. Zheng, Y. Miao and D. Zhang, *Small*, 2023, **19**, e2304032.
113 Z. Li, Y. Hu, K. A. Howard, T. Jiang, X. Fan, Z. Miao, Y. Sun, F. Besenbacher and M. Yu, *ACS Nano*, 2016, **10**, 984–997.
114 H. Nosrati, J. Charmi, M. Salehiabar, F. Abhari and H. Danafar, *ACS Biomater. Sci. Eng.*, 2019, **5**, 4416–4424.
115 S. Javani, M. Barsbay, M. Ghaffarlou, N. Mousazadeh, A. Mohammadi, F. Mozafari, H. Rezaeejam, L. Nasehi, H. Nosrati, T. Kavetskyy and H. Danafar, *J. Drug Delivery Sci. Technol.*, 2022, **71**, 103336.
116 L. Zhang, Q. Chen, X. Zou, J. Chen, L. Hu, Z. Dong, J. Zhou, Y. Chen, Z. Liu and L. Cheng, *J. Mater. Chem. B*, 2019, **7**, 5170–5181.
117 M. H. Faghfoori, H. Nosrati, H. Rezaeejam, J. Charmi, S. Kaboli, B. Johari and H. Danafar, *Int. J. Pharm.*, 2020, **582**, 119320.
118 S. Azizi, H. Nosrati, A. Sharafi and H. Danafar, *Appl. Organomet. Chem.*, 2020, **34**, e5251.
119 H. Yu, Y. Yang, T. Jiang, X. Zhang, Y. Zhao, G. Pang, Y. Feng, S. Zhang, F. Wang, Y. Wang, Y. Wang and L. W. Zhang, *ACS Appl. Mater. Interfaces*, 2019, **11**, 27536–27547.
120 Y. Wang, Y. Wu, Y. Liu, J. Shen, L. Lv, L. Li, L. Yang, J. Zeng, Y. Wang, L. W. Zhang, Z. Li, M. Gao and Z. Chai, *Adv. Funct. Mater.*, 2016, **26**, 5335–5344.
121 H. Nosrati, M. Salehiabar, F. Mozafari, J. Charmi, N. Erdoğan, M. Ghaffarlou, F. Abhari, H. Danafar, A. Ramazani and Y. Nuri Ertas, *Appl. Organomet. Chem.*, 2022, **36**, e6861.
122 H. Nosrati, F. Abhari, J. Charmi, M. Rahmati, B. Johari, S. Azizi, H. Rezaeejam and H. Danafar, *Artif. Cells, Nanomed., Biotechnol.*, 2019, **47**, 3832–3838.
123 B. Colak and Y. N. Ertas, *ACS Appl. Mater. Interfaces*, 2024, **16**, 15718–15729.
124 Y. Choghazardi, H. Azimian, A. M. Abadi, M. M. Khoshisani, F. V. Nezamdoust and H. Gholamhosseinian, *J. Nanomater.*, 2023, **2023**, 1–11.
125 H. Yu, Y. Yang, T. Jiang, X. Zhang, Y. Zhao, G. Pang, Y. Feng, S. Zhang, F. Wang, Y. Wang, Y. Wang and

L. W. Zhang, *ACS Appl. Mater. Interfaces*, 2019, **11**, 27536–27547.
126 D. Wang, Y. Yao, J. He, X. Zhong, B. Li, S. Rao, H. Yu, S. He, X. Feng, T. Xu, B. Yang, T. Yong, L. Gan, J. Hu and X. Yang, *Adv. Sci.*, 2020, **7**, 1901293.
127 S. Badrigilan, B. Shaabani, N. Gharehaghaji and A. Mesbahi, *Photodiagn. Photodyn. Ther.*, 2019, **25**, 504–514.
128 Y. Xuan, X.-L. Song, X.-Q. Yang, R.-Y. Zhang, Z.-Y. Song, D.-H. Zhao, X.-L. Hou, J. An, X.-S. Zhang and Y.-D. Zhao, *Chem. Eng. J.*, 2019, **375**, 122000.
129 J. Du, H. Ding, S. Fu, D. Li and B. Yu, *Front. Bioeng. Biotechnol.*, 2023, **10**, 1098923.
130 S. Goel, D. Ni and W. Cai, *ACS Nano*, 2017, **11**, 5233–5237.
131 L. R. H. Gerken, M. E. Gerdes, M. Pruschy and I. K. Herrmann, *Mater. Horiz.*, 2023, **10**, 4059–4082.
132 J. Li and H. Wang, *Nanoscale Horiz.*, 2023, **8**, 1155–1173.
133 B. Chen, C. Zhang, W. Wang, Z. Chu, Z. Zha, X. He, W. Zhou, T. Liu, H. Wang and H. Qian, *ACS Nano*, 2020, **14**, 14919–14928.
134 P. Jia, H. Ji, S. Liu, R. Zhang, F. He, L. Zhong and P. Yang, *J. Mater. Chem. B*, 2021, **9**, 101–111.
135 X. Meng, J. Liu, Q. Zheng, S. Li, H. Xiao, J. Huang, L. Ma, Y. Liu and J. Tang, *ACS Appl. Mater. Interfaces*, 2023, **15**, 58041–58053.
136 F. Abhari, J. Charmi, H. Rezaeejam, Z. Karimimoghaddam, H. Nosrati, H. Danafar and A. Farajollahi, *ACS Sustainable Chem. Eng.*, 2020, **8**, 5260–5269.
137 F. Wu, H. Chen, R. Liu, Y. Suo, Q. Li, Y. Zhang, H. Liu, Z. Cheng and Y. Chang, *Adv. Healthcare Mater.*, 2022, **11**, 2200809.
138 Z. Li, X. Fan, J. Liu, Y. Hu, Y. Yang, Z. Li, Y. Sun, C. Chen and M. Yu, *Nanomedicine*, 2018, **13**, 2283–2300.
139 B. Li, Y. Cheng, R. Zheng, X. Wu, F. Qi, Y. Wu, Y. Hu and X. Li, *J. Mater. Chem. B*, 2020, **8**, 8803–8808.
140 L. Dong, P. Zhang, X. Liu, R. Deng, K. Du, J. Feng and H. Zhang, *ACS Appl. Mater. Interfaces*, 2019, **11**, 7774–7781.
141 K. Song, J. Du, X. Wang, L. Zheng, R. Ouyang, Y. Li, Y. Miao and D. Zhang, *Adv. Healthcare Mater.*, 2022, **11**, 2102503.
142 S. Wen, W. Zhang, J. Yang, Z. Zhou, Q. Xiang and H. Dong, *ACS Nano*, 2024, **18**, 23672–23683.
143 Y. Dong, S. Dong, B. Liu, C. Yu, J. Liu, D. Yang, P. Yang and J. Lin, *Adv. Mater.*, 2021, **33**, 2106838.
144 A. Bijelic, M. Aureliano and A. Rompel, *Angew. Chem., Int. Ed.*, 2019, **58**, 2980–2999.
145 F. Carvalho and M. Aureliano, *Int. J. Mol. Sci.*, 2023, **24**, 5043.
146 R. Zhou, H. Wang, Y. Yang, C. Zhang, X. Dong, J. Du, L. Yan, G. Zhang, Z. Gu and Y. Zhao, *Biomaterials*, 2019, **189**, 11–22.
147 C. Orellana-Tavra, M. Köppen, A. Li, N. Stock and D. Fairen-Jimenez, *ACS Appl. Mater. Interfaces*, 2020, **12**, 5633–5641.
148 R. Zhou, X. Liu, Y. Wu, H. Xiang, J. Cao, Y. Li, W. Yin, Y. Zu, J. Li, R. Liu, F. Zhao, Z. Liu, C. Chen, Z. Gu, L. Yan and Y. Zhao, *ACS Nano*, 2020, **14**, 13016–13029.
149 S. A. Anushya, S. Prabhu, V. Ravikumar and A. Philominal, *J. Inorg. Organomet. Polym. Mater.*, 2023, **33**, 1369–1380.
150 R. Dou, Z. Du, T. Bao, X. Dong, X. Zheng, M. Yu, W. Yin, B. Dong, L. Yan and Z. Gu, *Nanoscale*, 2016, **8**, 11531–11542.
151 Y. Zhang, H. Zhang, Y. Wang, H. Wu, B. Zeng, Y. Zhang, Q. Tian and S. Yang, *J. Mater. Chem. B*, 2017, **5**, 1846–1855.
152 Y. Yao, P. Li, J. He, D. Wang, J. Hu and X. Yang, *ACS Appl. Mater. Interfaces*, 2021, **13**, 28650–28661.
153 H. Zhao, J. Wang, X. Li, Y. Li, C. Li, X. Wang, J. Wang, S. Guan, Y. Xu, G. Deng, Y. Chen, J. Lu and X. Liu, *J. Colloid Interface Sci.*, 2021, **604**, 80–90.
154 Y. Yao, P. Li, J. He, D. Wang, J. Hu and X. Yang, *ACS Appl. Mater. Interfaces*, 2021, **13**, 28650–28661.
155 J. Liu, J. Zhang, K. Song, J. Du, X. Wang, J. Liu, B. Li, R. Ouyang, Y. Miao, Y. Sun and Y. Li, *Small*, 2021, **17**, e2101015.
156 H. Nosrati, M. Ghaffarlou, M. Salehiabar, N. Mousazadeh, F. Abhari, M. Barsbay, Y. N. Ertas, H. Rashidzadeh, A. Mohammadi, L. Nasehi, H. Rezaeejam, S. Davaran, A. Ramazani, J. Conde and H. Danafar, *Biomater. Adv.*, 2022, **140**, 213090.
157 A. Rajaee, S. Wang, L. Zhao, D. Wang, Y. Liu, J. Wang and K. Ying, *Phys. Med. Biol.*, 2019, **64**, 195007.
158 A. Detappe, E. Thomas, M. W. Tibbitt, S. Kunjachan, O. Zavidij, N. Parnandi, E. Reznichenko, F. Lux, O. Tillement and R. Berbeco, *Nano Lett.*, 2017, **17**, 1733–1740.
159 R. Zhang, X. Wang, Y. Zhang, Q. Liu, H. Shen, B. Chen, C. Tan, W. Liu and X. Jin, *ACS Appl. Nano Mater.*, 2024, **7**, 11871–11881.
160 L. Zeng, H. Zhao, Y. Zhu, S. Chen, Y. Zhang, D. Wei, J. Sun and H. Fan, *J. Mater. Chem. B*, 2020, **8**, 4093–4105.
161 A. Ingham, L. Wharton, T. El Sayed, L. Southcott, B. L. McNeil, M. B. Ezhova, B. O. Patrick, M. D. G. Jaraquemada-Peláez and C. Orvig, *Inorg. Chem.*, 2022, **61**, 9119–9137.
162 K. A. Morgan, S. E. Rudd, A. Noor and P. S. Donnelly, *Chem. Rev.*, 2023, **123**, 12004–12035.
163 R. Eychenne, M. Chérel, F. Haddad, F. Guérard and J.-F. Gestin, *Pharmaceutics*, 2021, **13**, 906.
164 M. G. Ferrier, V. Radchenko and D. S. Wilbur, *Radiochim. Acta*, 2019, **107**, 1065–1085.
165 D. Szücs, J. P. Szabó, V. Arató, B. Gyuricza, D. Szikra, I. Tóth, Z. Képes, G. Trencsényi and A. Fekete, *Pharmaceuticals*, 2023, **16**, 1280.
166 S. Hassfjell, K. Ingebrigtsen and Ø. S. Bruland, *Nucl. Med. Biol.*, 2001, **28**, 425–433.
167 I. n. d. services, **https://www-nds.iaea.org/**, (accessed 21st of August, 2024).
168 G. Henriksen and P. Hoff, *Appl. Radiat. Isot.*, 1998, **49**, 357–359.

169 S. Ahenkorah, I. Cassells, C. M. Deroose, T. Cardinaels, A. R. Burgoyne, G. Bormans, M. Ooms and F. Cleeren, *Pharmaceutics*, 2021, **13**, 599.
170 S. Franchi, V. Di Marco and M. Tosato, *Nucl. Med. Biol.*, 2022, **114–115**, 168–188.
171 L. Wharton, C. Zhang, H. Yang, J. Zeisler, V. Radchenko, C. Rodríguez-Rodríguez, M. Osooly, B. O. Patrick, K.-S. Lin, F. Bénard, P. Schaffer and C. Orvig, *Bioconjugate Chem.*, 2022, **33**, 505–522.
172 J. Šimeček, P. Hermann, C. Seidl, F. Bruchertseifer, A. Morgenstern, H.-J. Wester and J. Notni, *EJNMMI Res.*, 2018, **8**, 78.
173 A. Hu, V. Brown, S. N. Macmillan, V. Radchenko, H. Yang, L. Wharton, C. F. Ramogida and J. J. Wilson, *Inorg. Chem.*, 2022, **61**, 801–806.
174 P. Randhawa, K. J. Kadassery, B. L. McNeil, S. N. MacMillan, L. Wharton, H. Yang, J. J. Wilson and C. F. Ramogida, *Inorg. Chem.*, 2024, **63**, 21177–21193.
175 F. Bruchertseifer, P. Comba, B. Martin, A. Morgenstern, J. Notni, M. Starke and H. Wadepohl, *ChemMedChem*, 2020, **15**, 1591–1600.
176 I. Kopp, P. Cieslik, K. Anger, T. Josephy, L. Neupert, G. Velmurugan, M. Gast, H. Wadepohl, S. A. Brühlmann, M. Walther, K. Kopka, M. Bachmann, H. Stephan, M. Kubeil and P. Comba, *Inorg. Chem.*, 2023, **62**, 20754–20768.
177 H. Song, M. Hedayati, R. F. Hobbs, C. Shao, F. Bruchertseifer, A. Morgenstern, T. L. Deweese and G. Sgouros, *Mol. Cancer Ther.*, 2013, **12**, 2043–2054.
178 M. Lingappa, H. Song, S. Thompson, F. Bruchertseifer, A. Morgenstern and G. Sgouros, *Cancer Res.*, 2010, **70**, 6815–6823.
179 E. Revskaya, Z. Jiang, A. Morgenstern, F. Bruchertseifer, M. Sesay, S. Walker, S. Fuller, M. S. Lebowitz, C. Gravekamp, H. A. Ghanbari and E. Dadachova, *Cancer Biother. Radiopharm.*, 2017, **32**, 57–65.
180 M. E. Autenrieth, C. Seidl, F. Bruchertseifer, T. Horn, F. Kurtz, B. Feuerecker, C. D'Alessandria, C. Pfob, S. Nekolla, C. Apostolidis, S. Mirzadeh, J. E. Gschwend, M. Schwaiger, K. Scheidhauer and A. Morgenstern, *Eur. J. Nucl. Med. Mol. Imaging*, 2018, **45**, 1364–1371.
181 S. Heskamp, R. Hernandez, J. D. M. Molkenboer-Kuenen, M. Essler, F. Bruchertseifer, A. Morgenstern, E. J. Steenbergen, W. Cai, C. Seidl, W. J. McBride, D. M. Goldenberg and O. C. Boerman, *J. Nucl. Med.*, 2017, **58**, 926–933.
182 D. E. Milenic, E. D. Brady, K. Garmestani, P. S. Albert, A. Abdulla and M. W. Brechbiel, *Cancer*, 2010, **116**, 1059–1066.
183 L. Królicki, F. Bruchertseifer, J. Kunikowska, H. Koziara, B. Królicki, M. Jakuciński, D. Pawlak, C. Apostolidis, S. Mirzadeh, R. Rola, A. Merlo and A. Morgenstern, *Eur. J. Nucl. Med. Mol. Imaging*, 2019, **46**, 614–622.
184 E. Drecoll, F. C. Gaertner, M. Miederer, B. Blechert, M. Vallon, J. M. Müller, A. Alke, C. Seidl, F. Bruchertseifer, A. Morgenstern, R. Senekowitsch-Schmidtke and M. Essler, *PLoS One*, 2009, **4**, e5715.
185 J. D. Nosanchuk, A. Jeyakumar, A. Ray, E. Revskaya, Z. Jiang, R. A. Bryan, K. J. H. Allen, R. Jiao, M. E. Malo, B. L. Gómez, A. Morgenstern, F. Bruchertseifer, D. Rickles, G. B. Thornton, A. Bowen, A. Casadevall and E. Dadachova, *Sci. Rep.*, 2018, **8**, 5466.
186 B. J. Allen, C. Raja, S. Rizvi, Y. Li, W. Tsui, P. Graham, J. Thompson, R. Reisfeld, J. Kearsley, A. Morgenstern and C. Apostolidis, *Cancer Biol. Ther.*, 2005, **4**, 1318–1324.
187 C. Raja, P. Graham, S. Rizvi, E. Song, H. Goldsmith, J. Thompson, A. Bosserhoff, A. Morgenstern, C. Apostolidis, J. Kearsley, R. Reisfeld and B. J. Allen, *Cancer Biol. Ther.*, 2007, **6**, 846–852.
188 B. J. Allen, A. A. Singla, S. M. A. Rizvi, P. Graham, F. Bruchertseifer, C. Apostolidis and A. Morgenstern, *Immunotherapy*, 2011, **3**, 1041–1050.
189 J. Ménager, J.-B. Gorin, C. Maurel, L. Drujont, S. Gouard, C. Louvet, M. Chérel, A. Faivre-Chauvet, A. Morgenstern, F. Bruchertseifer, F. Davodeau, J. Gaschet and Y. Guilloux, *PLoS One*, 2015, **10**, e0130249.
190 N. Fichou, S. Gouard, C. Maurel, J. Barbet, L. Ferrer, A. Morgenstern, F. Bruchertseifer, A. Faivre-Chauvet, E. Bigot-Corbel, F. Davodeau, J. Gaschet and M. Chérel, *Front. Med.*, 2015, **2**, 76.
191 K. Teiluf, C. Seidl, B. Blechert, F. C. Gaertner, K.-P. Gilbertz, V. Fernandez, F. Bassermann, J. Endell, R. Boxhammer, S. Leclair, M. Vallon, M. Aichler, A. Feuchtinger, F. Bruchertseifer, A. Morgenstern and M. Essler, *Oncotarget*, 2015, **6**, 4692–4703.
192 S. I. Park, J. Shenoi, J. M. Pagel, D. K. Hamlin, D. S. Wilbur, N. Orgun, A. L. Kenoyer, S. Frayo, A. Axtman, T. Bäck, Y. Lin, D. R. Fisher, A. K. Gopal, D. J. Green and O. W. Press, *Blood*, 2010, **116**, 4231–4239.
193 M. Roscher, I. Hormann, O. Leib, S. Marx, J. Moreno, E. Miltner and C. Friesen, *Oncotarget*, 2013, **4**, 218–230.
194 A. Derrien, S. Gouard, C. Maurel, M.-H. Gaugler, F. Bruchertseifer, A. Morgenstern, A. Faivre-Chauvet, J.-M. Classe and M. Chérel, *Front. Med.*, 2015, **2**(88).
195 A. Gustafsson-Lutz, T. Bäck, E. Aneheim, R. Hultborn, S. Palm, L. Jacobsson, A. Morgenstern, F. Bruchertseifer, P. Albertsson and S. Lindegren, *EJNMMI Res.*, 2017, **7**, 38.
196 A. M. E. Gustafsson, T. Bäck, J. Elgqvist, L. Jacobsson, R. Hultborn, P. Albertsson, A. Morgenstern, F. Bruchertseifer, H. Jensen and S. Lindegren, *Nucl. Med. Biol.*, 2012, **39**, 15–22.
197 D. Horváth, A. Vágner, D. Szikra, G. Trencsényi, N. Demitri, N. Guidolin, A. Maiocchi, S. Ghiani, F. Travagin, G. B. Giovenzana and Z. Baranyai, *Angew. Chem., Int. Ed.*, 2022, **61**, e202207120.
198 H. S. Chan, M. W. Konijnenberg, T. Daniels, M. Nysus, M. Makvandi, E. De Blois, W. A. Breeman, R. W. Atcher, M. De Jong and J. P. Norenberg, *EJNMMI Res.*, 2016, **6**, 83.
199 C. Kratochwil, F. L. Giesel, F. Bruchertseifer, W. Mier, C. Apostolidis, R. Boll, K. Murphy, U. Haberkorn and

A. Morgenstern, *Eur. J. Nucl. Med. Mol. Imaging*, 2014, **41**, 2106–2119.
200 S. H. Kurtzman, A. Russo, J. B. Mitchell, W. Degraff, W. F. Sindelar, M. W. Brechbiel, O. A. Gansow, A. M. Friedman, J. J. Hines, J. Gamson and R. W. Atcher, *JNCI, J. Natl. Cancer Inst.*, 1988, **80**, 449–452.
201 R. Jiao, K. J. H. Allen, M. E. Malo, M. Helal, Z. Jiang, K. Smart, S. V. Buhl, D. Rickles, R. A. Bryan and E. Dadachova, *Cancer Med.*, 2019, **8**, 5289–5300.
202 B. J. Allen, S. M. A. Rizvi, C. F. Qu and R. C. Smith, *Cancers*, 2011, **3**, 1821–1843.
203 Y. Li, S. M. A. Rizvi, M. Ranson and B. J. Allen, *Br. J. Cancer*, 2002, **86**, 1197–1203.
204 D. Cordier, F. Forrer, F. Bruchertseifer, A. Morgenstern, C. Apostolidis, S. Good, J. Müller-Brand, H. Mäcke, J. C. Reubi and A. Merlo, *Eur. J. Nucl. Med. Mol. Imaging*, 2010, **37**, 1335–1344.
205 L. Krolicki, F. Bruchertseifer, J. Kunikowska, H. Koziara, B. Królicki, M. Jakuciński, D. Pawlak, C. Apostolidis, S. Mirzadeh, R. Rola, A. Merlo and A. Morgenstern, *Eur. J. Nucl. Med. Mol. Imaging*, 2018, **45**, 1636–1644.
206 J. G. Jurcic, S. M. Larson, G. Sgouros, M. R. McDevitt, R. D. Finn, C. R. Divgi, Å. M. Ballangrud, K. A. Hamacher, D. Ma, J. L. Humm, M. W. Brechbiel, R. Molinet and D. A. Scheinberg, *Blood*, 2002, **100**, 1233–1239.
207 T. L. Rosenblat, M. R. McDevitt, D. A. Mulford, N. Pandit-Taskar, C. R. Divgi, K. S. Panageas, M. L. Heaney, S. Chanel, A. Morgenstern, G. Sgouros, S. M. Larson, D. A. Scheinberg and J. G. Jurcic, *Clin. Cancer Res.*, 2010, **16**, 5303–5311.
208 Y. Dekempeneer, V. Caveliers, M. Ooms, D. Maertens, M. Gysemans, T. Lahoutte, C. Xavier, Q. Lecocq, K. Maes, P. Covens, B. W. Miller, F. Bruchertseifer, A. Morgenstern, T. Cardinaels and M. D'Huyvetter, *Mol. Pharm.*, 2020, **17**, 3553–3566.
209 C. Kratochwil, K. Schmidt, A. Afshar-Oromieh, F. Bruchertseifer, H. Rathke, A. Morgenstern, U. Haberkorn and F. L. Giesel, *Eur. J. Nucl. Med. Mol. Imaging*, 2018, **45**, 31–37.
210 M. Sathekge, O. Knoesen, M. Meckel, M. Modiselle, M. Vorster and S. Marx, *Eur. J. Nucl. Med. Mol. Imaging*, 2017, **44**, 1099–1100.
211 M. D. Diener, J. M. Alford, S. J. Kennel and S. Mirzadeh, *J. Am. Chem. Soc.*, 2007, **129**, 5131–5138.
212 R. Wang, H. T. Wolterbeek and A. G. Denkova, *J. Label. Compd. Radiopharm.*, 2024, **67**, 375–383.
213 N. Kauffman, S. K. Singh, J. Morrison and K. R. Zinn, *Front. Chem.*, 2023, **11**, 1204872.
214 Z. Cao, K. Deng, J. Jiang, K. Tian and B. Wang, *Biomed. Pharmacother.*, 2025, **182**, 117727.
215 Y. Sun, L. Liu, H. He, G. Cui, Y. Zheng, C. Ye, L. Qu, Y. Sun, J. Ji, T. Lammers, Y. Zhang and Z. Zhong, *J. Controlled Release*, 2025, **379**, 327–343.
216 J. Li, C. Tan, J. Yang, Z. Xiang, Y. Wang, M. Shen, S. Zhu, T. He, X. Liang, B. Shao, H. Li, Z. Li, L. Liu and C. Gong, *Biomaterials*, 2025, **316**, 123005.
217 C. Arndt, R. Bergmann, F. Striese, K. Merkel, D. Máthé, L. R. Loureiro, N. Mitwasi, A. Kegler, F. Fasslrinner, K. E. González Soto, C. Neuber, N. Berndt, N. Kovács, D. Szöllősi, N. Hegedűs, G. Tóth, J.-P. Emmermann, K. B. Harikumar, T. Kovacs, M. Bachmann and A. Feldmann, *Cancers*, 2022, **14**, 1996.
218 A. S. Köseer, L. R. Loureiro, J. Jureczek, N. Mitwasi, K. E. González Soto, J. Aepler, T. Bartsch, A. Feldmann, L. A. Kunz-Schughart, A. Linge, M. Krause, M. Bachmann, C. Arndt and A. Dubrovska, *Cancers*, 2022, **14**, 1677.
219 C. Arndt, L. R. Loureiro, A. Feldmann, J. Jureczek, R. Bergmann, D. Máthé, N. Hegedüs, N. Berndt, S. Koristka, N. Mitwasi, F. Fasslrinner, C. Lamprecht, A. Kegler, A. Hoffmann, T. Bartsch, A. S. Köseer, G. Egan, M. Schmitz, V. Hořejší, M. Krause, A. Dubrovska and M. Bachmann, *OncoImmunology*, 2020, **9**, 1743036.
220 L. R. Loureiro, L. Hoffmann, C. Neuber, L. Rupp, C. Arndt, A. Kegler, M. Kubeil, C. E. Hagemeyer, H. Stephan, M. Schmitz, A. Feldmann and M. Bachmann, *J. Exp. Clin. Cancer Res.*, 2023, **42**, 341.
221 M. Bachmann, *Immunol. Lett.*, 2019, **211**, 13–22.
222 P. Valent, B. Groner, U. Schumacher, G. Superti-Furga, M. Busslinger, R. Kralovics, C. Zielinski, J. M. Penninger, D. Kerjaschki, G. Stingl, J. S. Smolen, R. Valenta, H. Lassmann, H. Kovar, U. Jäger, G. Kornek, M. Müller and F. Sörgel, *J. Innate Immun.*, 2016, **8**, 111–120.
223 M. J. Smyth and M. W. Teng, *Clin. Transl. Immunol.*, 2018, **7**, e1041.
224 A. Patterson and N. Auslander, *Nat. Commun.*, 2022, **13**, 5151.
225 C. Arndt, F. Fasslrinner, L. R. Loureiro, S. Koristka, A. Feldmann and M. Bachmann, *Cancers*, 2020, **12**, 1302.
226 G. Gross, T. Waks and Z. Eshhar, *Proc. Natl. Acad. Sci. U. S. A.*, 1989, **86**, 10024–10028.
227 C. Arndt, A. Feldmann, S. Koristka, M. Cartellieri, M. Dimmel, A. Ehninger, G. Ehninger and M. Bachmann, *Prostate*, 2014, **74**, 1335–1346.
228 M. Bachmann, *US patent* 10246516B2, 2016.
229 M. Bachmann, *US patent* 10766943, 2020.
230 M. Bachmann, *US patent* 17/251447, 2021.
231 M. Cartellieri, A. Feldmann, S. Koristka, C. Arndt, S. Loff, A. Ehninger, M. Von Bonin, E. P. Bejestani, G. Ehninger and M. P. Bachmann, *Blood Cancer J.*, 2016, **6**, e458–e458.
232 A. Feldmann, A. Hoffmann, R. Bergmann, S. Koristka, N. Berndt, C. Arndt, L. Rodrigues Loureiro, E. Kittel-Boselli, N. Mitwasi, A. Kegler, C. Lamprecht, K. E. González Soto and M. Bachmann, *OncoImmunology*, 2020, **9**, 1785608.
233 L. E. Pelepenko, A. C. P. Janini, B. P. F. A. Gomes, A. De-Jesus-Soares and M. A. Marciano, *Antibiotics*, 2022, **11**, 1741.
234 M. Epple, V. M. Rotello and K. Dawson, *Acc. Chem. Res.*, 2023, **56**, 3369–3378.
235 S. Li, C. Cortez-Jugo, Y. Ju and F. Caruso, *ACS Nano*, 2024, **18**, 33257–33263.

236 C. Domingues, A. Santos, C. Alvarez-Lorenzo, A. Concheiro, I. Jarak, F. Veiga, I. Barbosa, M. Dourado and A. Figueiras, *ACS Nano*, 2022, **16**, 9994–10041.
237 R. Prasad, A. Ghosh, V. Patel, B. Peng, B. B. Mendes, E. H. A. Win, L. G. Delogu, J. Y. Wong, K. J. Pischel, J. R. Bellare, A. Bar-Shir, A. S. Thakor, W. J. Parak, Z. M. Bhujwalla, Y. S. Zhang, N. Kommineni, V. M. Rotello, W. Cai, T. Lammers, T. W. Odom, G. Padmanaban, D. Peer, J. F. Lovell, R. Srivastava, R. Langer and J. Conde, *ACS Nano*, 2025, **19**, 2979–2991.